UNIVERSITY OF LEEDS

This is a repository copy of *Recognition of melferite – A rock formed in syn-deformational high-strain melt-transfer zones through sub-solidus rocks: A review and synthesis of microstructural criteria*.

White Rose Research Online URL for this paper:
https://eprints.whiterose.ac.uk/190743/

Version: Accepted Version

Article:

Daczko, NR and Piazolo, S orcid.org/0000-0001-7723-8170 (2022) Recognition of melferite – A rock formed in syn-deformational high-strain melt-transfer zones through sub-solidus rocks: A review and synthesis of microstructural criteria. Lithos, 430-431. 106850. p. 1. ISSN 0024-4937

https://doi.org/10.1016/j.lithos.2022.106850

© 2022 Elsevier B.V. Licensed under the Creative Commons Attribution-NonCommercial-NoDerivatives 4.0 International License (http://creativecommons.org/licenses/by-nc-nd/4.0/).

Reuse
Items deposited in White Rose Research Online are protected by copyright, with all rights reserved unless indicated otherwise. They may be downloaded and/or printed for private study, or other acts as permitted by national copyright laws. The publisher or other rights holders may allow further reproduction and re-use of the full text version. This is indicated by the licence information on the White Rose Research Online record for the item.

Takedown
If you consider content in White Rose Research Online to be in breach of UK law, please notify us by emailing eprints@whiterose.ac.uk including the URL of the record and the reason for the withdrawal request.

White Rose university consortium
Universities of Leeds, Sheffield & York

eprints@whiterose.ac.uk
https://eprints.whiterose.ac.uk/

Revised Manuscript with No changes marked
Click here to view linked References
Click here to access/download;Revised Manuscript with No changes marked;Daczko&PiazoloR1_clean.docx

Recognition of melferite – a rock formed in syn-deformational high-strain melt-transfer zones through sub-solidus rocks: a review and synthesis of microstructural criteria

Nathan R. Daczko[1] and Sandra Piazolo[2]

Corresponding Author: nathan.daczko@mq.edu.au

[1] Australian Research Council Centre of Excellence for Core to Crust Fluid Systems (CCFS) and GEMOC, School of Natural Sciences, Macquarie University, NSW 2109 Australia.

[2] School of Earth and Environment, University of Leeds, Leeds, UK.

Keywords: high-strain zone, mylonite, melt-present deformation, shear zone, microstructures, melt migration and ascent

Abstract

Melt transfer and migration occurs through both supra- and sub-solidus rocks. Mechanisms of melt transfer include dyking, mobile hydrofracturing and diffuse porous melt flow where melt flow may or may not be channelized via instabilities or into high-strain zones of active deformation. Here, we highlight the microstructural- and outcrop-scale signatures of syn-deformational melt-migration pathways through high-strain zones that cut sub-solidus rocks. High-strain zones with high proportions (> 10%) of macroscopic, internally undeformed, felsic or leucocratic material are readily interpreted as important melt-migration pathways and are most common in supra-solidus host rocks. However, it is challenging to recognise high-strain melt-migration pathways through sub-solidus rocks; these pathways may lack noticeable felsic or leucocratic components at the outcrop scale and share many macroscopic features in common with 'classic' sub-solidus mylonite, such that the two are generally conflated. We contrast field and microstructural characteristics of 'classic' mylonite originating from solid-state deformation with those of high-strain zones that also cut sub-solidus rocks yet have microstructural indicators of the former presence of melt. We compile several features allowing one to distinguish solid-state from melt-present deformation in high-strain zones that cut sub-solidus rocks. Our aim is to encourage geologists to assess such high-strain zones on a case-by-case basis, in view of sub-solidus (i.e., mylonitic) versus melt-present deformation. Such assessment is crucial as (1) rocks deformed in the presence of melt, even small percentages of melt, are orders of magnitude

weaker than their solid-state equivalents, (2) melt-rock interaction in such zones may result in metasomatism, and (3) such zones may sustain long-lived melt migration and ascent enabling chemical differentiation at a crustal scale. With this contribution we aim to increase the ease of recognizing this important subset of melt-migration pathways by assisting in clarity of description and interpretation of high-strain rocks.

Introduction

Compositionally varied partial melts are generated in the mantle and/or crust in all geodynamic settings. The presence and chemical signatures of volcanoes reveal that melt must commonly ascend from deep in the Earth to its surface (e.g., Tanton et al. 2001, Aldanmaz et al. 2006). The processes that move melt from source to sink involve segregation, extraction, migration, and accumulation (Brown, 1994, 2013; Sawyer, 1994; Rutter & Neuman, 1995; Etheridge et al., 2021). At or close to the source, melt migration pathways likely occur in supra-solidus rocks. They are thought to be initially dispersed, and coalesce into channelled pathways (Etheridge et al., 2021). Different to melt migration in supra-solidus rocks, melt transfer through sub-solidus country rocks requires rapid ascent in focussed melt-migration pathways to prevent cooling and crystallization. High-strain zones are an example of such sites of focussed melt flow. It has been shown that high-strain zones may act as important melt migration pathways – they are recognized in the field as high-strain zones containing high proportions (> 10%) of macroscopic, internally undeformed, felsic or leucocratic material that is inferred to, at least in part, represent the crystallisation of former melt (Tommasi et al., 1994; Brown & Solar, 1998a; Marchildon & Brown, 2003; Weinberg & Mark, 2008; Schulmann et al., 2008; Hasalova et al., 2011; Carvalho et al., 2016, 2017; Piazolo et al., 2020). However, if melt-bearing high-strain zones cut sub-solidus rocks but lack noticeable felsic or leucocratic components at the outcrop scale (e.g., dykes and lenses), they are challenging to recognise as melt-migration pathways (e.g., Stuart et al., 2018a,b; Gardner et al., 2020). Additionally, these pathways share many macroscopic features in common with 'classic' sub-solidus mylonite, such that the two may be easily conflated (compare Figs. 1 & 2).

The recognition of such dynamic melt-migration pathways through sub-solidus rocks is significant, as these represent not only zones of major rheological weakening, due to a combination of factors that may include grain size reduction, reaction softening, and enhanced melt-assisted deformation mechanisms (e.g., Arzi, 1978; Hollister & Crawford, 1986; Dell'Angelo & Tullis, 1988; Davidson et al., 1994; Rutter & Neumann, 1995; Paterson et al., 1998; Piazolo et al., 2020), but are potentially also zones of significant, long-lived melt migration and ascent enabling chemical differentiation at a crustal scale (e.g., Clemens & Mawer, 1992; Brown, 1994; Brown & Rushmer, 1997; Sawyer, 2001).

This contribution focuses on the microstructure of high-strain zones that cut sub-solidus rocks with the objective to separate high-strain zones into those that form in the solid-state versus those that act as syntectonic melt migration pathways. We contrast (1) established field and microstructural criteria used to identify solid-state high-strain zones (i.e., mylonite zones; Fig. 1) with (2) criteria suggested here for recognising high-strain deformation-assisted melt-migration pathways through sub-solidus rocks (Fig. 2). First, we briefly review the key characteristics of solid-state high-strain deformation followed by a broad overview of melt-present deformation, encompassing dykes, mobile hydrofractures, large scale magmatic flow, and deformation of rocks with high proportions of partial melt. We focus specifically on characteristics associated with deformation. In addition, we highlight the microstructural features used to infer the former presence of melt, established from igneous rocks and migmatites. This is followed by a brief review and synthesis of recent research that has recognised such microstructures in high-strain zones with two key features: (1) the high-strain zones lack field evidence commonly used to infer melt-present deformation, and (2) they cut sub-solidus rocks. We finish with a discussion of the importance of distinguishing between solid-state vs melt-present deformation in terms of strain localisation in dominantly sub-solidus rocks, chemical modification, and the efficiency of melt migration to encourage geologists to carefully assess high-strain zones, particularly where they cut sub-solidus wall rocks. As such, we hope to increase the recognition of high-strain melt-migration pathways, i.e., those where the evidence for the former presence of melt is visible at the thin section scale but not necessarily obvious at the outcrop scale.

Solid-state high-strain zones

Deformation is commonly localised into planar zones of high strain, recognised in the field by their strongly developed and regularly spaced planar foliation and most commonly a finer grain size relative to adjacent rocks, resulting in a change in colour (Fig. 1). Such high-strain zones accommodate relative movement of comparatively rigid surrounding rocks (e.g., White et al., 1980; Ramsay, 1980; Poirier, 1980; Hobbs et al. 1986; Jiang & Williams, 1998). Deformation within these zones results in the formation of new fabrics including foliation and lineation (Fig. 1), mineral assemblages, and other distinct structural features including folds (e.g., Carreras et al., 2005). Deflections ('drag folds') of pre-existing planar elements into the high-strain zone with a gradual change in fabric and foliation intensity are also common. Mineral assemblages and microstructures associated with the high-strain zone allow deduction of the conditions of deformation including temperature, pressure, strain rate, type of deformation and the presence of fluid (Tullis et al., 1982; Stipp et al. 2002; Passchier & Trouw, 2005). High-strain zones developed within solid-state rocks are broadly divided into those dominated by brittle or ductile deformation, forming the structurally- and process-defined rock types: *cataclasite* and *mylonite*, respectively.

Lapworth (1885) introduced the term *mylonite* for rocks occurring along the Moine Thrust, NW Scotland; a well-defined high-strain zone (Fig. 1a,b). He interpreted a cataclastic process involving strong grinding or milling of the Moine Schists in the high-strain zone, hence coined a term originating from the Greek *mylon*, meaning a mill. Christie (1963) identified widespread recrystallisation in the Moine mylonite, although he interpreted this as post-dating the cataclasis inferred by Lapworth. Subsequent work showed that many mylonitic rocks contain grains that are strongly distorted due to crystal-plastic deformation (Bell & Etheridge, 1973; Hobbs et al., 1976; Tullis et al., 1982). Current usage of mylonite is exclusively for rocks deformed by solid-state ductile deformation in which the "stress-supporting network is affected by crystal-plastic deformation" (e.g., Passchier & Trouw, 2005). Mylonite (sensu lato) with 10–50% matrix (fine-grained, recrystallised grains) is classified as *protomylonite* (e.g., Fig. 1f; 3c$_i$), while those rocks with 50–90% or >90% matrix are called *mylonite* (sensu stricto, e.g., Fig. 1d,e; 3a,b), or *ultramylonite*, respectively (e.g., Passchier & Trouw, 2005).

In the last two decades, it has become clear that high-strain zones may show microstructures indicative of either (1) crystal-plastic deformation and dislocation creep or (2) diffusion creep sensu lato. The first can be inferred from microstructural observation of undulous extinction, serrated or curved boundaries, bimodal grain size distribution, overall bulk grain size reduction, presence of subgrains and small new grains, and crystal preferred orientation. Diffusion creep sensu lato includes grain boundary sliding accommodated by diffusion and/or dislocation movement and dissolution-precipitation creep. Some high-strain zones may involve a combination of the two deformation regimes.

Compositional or grain size banding is common in mylonite (e.g., Fig. 1c,d). In many cases, high-strain rocks exhibit a well-developed object lineation (Piazolo & Passchier, 2002). Mylonitic high-strain zones exhibit a fabric gradient from host rock to high-strain zone which is commonly accompanied by a significant grain size reduction (Fig. 1b,c; Fig. 3b). Incomplete grain size reduction results in strong grain size variation typically involving porphyroclasts surrounded by a finer-grained matrix that are easily distinguished in the field and thin section (Fig. 1d–f; Fig. 3b_{i},c_{i}). Other key features in thin section have been identified and are expanded upon next (e.g., White et al., 1980; Lister & Snoke, 1984; Hobbs et al., 1986; Simpson & De Paor, 1993). The most conspicuous is a bimodal grain size distribution, with uniform small grains forming a matrix to larger, elongate grains that exhibit deformation lamellae and/or twins, undulose extinction and subgrains both at grain boundaries and cutting through grains (Fig. 3a_{ii},b_{ii}). So-called *core-and-mantle* structures or *mantled porphyroclasts*, where a large grain is surrounded by small, dynamically recrystallised grains of the same mineral, are common (Fig. 3a_{ii},c_{ii}; White, 1979). Medium- to high-grade deformation at low to intermediate strain rates forms curved to highly irregular grain boundaries that form window and pinning structures (Jessell, 1987; Passchier & Trouw, 2005), and the grain size distribution will tend to be less bimodal (e.g., Piazolo et al. 2002; de Freitas et al, 2021). In rocks that have undergone subsequent deformation during high grade metamorphism in the solid state, some of these microstructures may be erased (e.g., by recrystallisation of a former bimodal grain size distribution; e.g., Heilbronner & Tullis, 2002; Piazolo et al. 2006). Micro-folding (Fig. 3b_{i}) and shape-preferred or crystallographic-preferred orientation of minerals are also common in mylonitic rocks (e.g., Law, 1990). Elongate grains (particularly quartz) or quartz ribbons with very high aspect ratios which are several mm long and show a large number of grains or subgrains are observed particularly in high grade mylonites (Fig. 3a$_{iii}$, b$_{iii}$; e.g., Hippert et al., 2001; Bose & Sengupta, 2003). Furthermore, Commonly, stronger minerals deform in a brittle manner forming bands of rigid clasts “floating” in a ductile matrix (Fig. 3b$_{ii}$). Many microstructures are asymmetric and are useful shear-sense indicators (e.g., Hanmer & Passchier, 1991) including shear bands that are oblique to the main foliation (Fig. 1d,f; Lister & Snoke, 1984). Nevertheless, it should be noted that some mylonitic rocks may lack such asymmetric structures due to the deformation regime that the rock analysed was subjected to (e.g., Baily et al., 2007; Mukherjee, 2017).

Characteristic microstructures of diffusion creep and grain boundary sliding include very small grain sizes, presence of shape preferred orientation (lacking both crystallographic preferred orientation and undulous extinction), subgrain boundaries and necking high-strain zones (e.g., Svahnberg & Piazolo, 2010, Menegon et al., 2015). Signatures of dissolution-precipitation creep include grain indentations and truncations, grain flattening, enhanced compositional variations including insoluble seams, strain shadows or beards (e.g., Stokes et al., 2012).

Melt-transfer zones

Types and field characteristics

Dyke-like structures that may be continuous or discontinuous at the scale of an outcrop and mobile hydrofractures represent signatures of melt ascent through rocks which at the time of melt transfer were behaving in a brittle manner; dyking is an important mechanism of melt transfer, particularly in the upper crust (e.g., Holness & Watt 2002; Holness et al., 2005), and can either be passive i.e., flow of melt into an open gap or active by dynamic fracturing at the hydraulic head resulting in so-called mobile hydrofractures (e.g., Clemens and Mawer, 1992; Petford et al., 1994; Rubin, 1995; Clemens, 1998; Geshi, 2001; Bons et al., 2001; Kisters et al., 2009; Diener et al., 2014; Hall & Kisters, 2016). These geological structures are readily recognised in the field by their sharp cross-cutting relationships and their igneous microstructure closely resembling the igneous component of migmatites reviewed below.

The simplest scenario of melt-present deformation occurs during magmatic to submagmatic flow, involving deformation of crystal-rich magmatic systems. Key evidence of strain in supra-solidus magmatic systems includes: shape-preferred orientation of elongate crystals that are not internally deformed, or magmatic foliations that may be concordant with aligned enclave swarms and mafic schlieren (Vernon 1986; Paterson et al., 1989; Higgins 1998; Wiebe et al., 2002; Yoshinobu & Hirth 2002; Collins et al., 2006, Zibra et al. 2020), imbrication of elongate euhedral crystals that are not internally deformed (e.g., Vernon 2004; Paterson et al., 2005), insufficient solid-state strain around imbricated crystals if rotation had occurred in the solid state (Vernon, 2000), and strongly foliated and flattened enclaves lacking evidence of crystal-plastic deformation (e.g., Wiebe & Collins 1998). Magmatic flow with minimal solid-state deformation of crystals is inferred in all these cases (Vernon & Paterson, 2006), as the features are consistent with accommodation of strain by deformation of a melt phase (Vernon, 2000). These supra-solidus plutonic scenarios of melt-present deformation provide a framework to understanding how rocks behave during melt-present deformation, including brittle processes (e.g., Bouchez et al., 1992), and how the rock product contrasts to those deformed in the solid-state (Miller & Paterson, 1994; Vernon, 2000).

Rocks described as *stromatic migmatite* have been interpreted to represent zones of melt-transfer active during high-strain deformation (e.g. Park, 1983). These stromatic migmatites are characterised by numerous thin, parallel and laterally extensive layers or stroma of coarse grained, felsic material referred to as leucosome (Fig. 3a). The strongly layered morphology is attributed to transposition of leucosome during melt present high-strain deformation (Park, 1983), although stromatic migmatites have been shown to form in low-strain settings (Johannes & Gupta, 1982). Likewise, some kilometre-scale regions of stromatic migmatite hosted in diatexite (a migmatite with high melt fraction; Brown, 1973) have been interpreted as crustal-scale high-strain magma transfer zones involving migration and/or draining of melt (e.g., Sleep, 1974; Scott & Stevenson, 1986) from adjacent less deformed migmatite, i.e., supra-solidus wall rocks (Brown & Solar, 1998a; Marchildon & Brown, 2003; Weinberg & Mark, 2008; Schulmann et al., 2008; Hasalova et al., 2011). Field studies link melt ascent and eventual emplacement of plutons based on the close association between regional deformation, migmatisation, dyking, and zones of strain localisation (e.g., Pitcher, 1979; Castro, 1986; Hutton, 1988; Vigneresse, 1995; Brown and Solar, 1998b; de Saint Blanquat et al., 1998; Rosenburg, 2004; Vernon et al., 2012; Brown, 2013; Zibra et al., 2014).

Furthermore, as summarised by Cruden & Weinberg (2018), faults and shear zones from all geodynamic systems have been implicated as high-strain melt-migration pathways through both supra- and sub-solidus rocks (normal (e.g., Richards & Collins, 2004; Grocott & Taylor, 2002; Grocott et al., 1994, 2009; Hutton et al., 1990; Gardner et al., 2020), thrust/reverse (e.g., Ingram & Hutton, 1994; Collins & Sawyer, 1996; Stuart et al., 2018a,b; Piazolo et al., 2020; Silva et al., 2022), strike-slip (e.g., Guineberteau et al., 1987; Hutton, 1988; Tikoff & Teyssier, 1992), transpressional systems (e.g., McCaffrey, 1992; Brown & Solar, 1998b; Benn et al., 1999; Denèle et al., 2008; Vernon et al., 2012).

In all of the above cases, syn-deformational melt-transfer zones through both supra- and sub-solidus rocks have been recognized as such primarily based on observed structural offsets and the preservation of high proportions (>10%) of internally undeformed felsic or leucocratic material identifiable as igneous components in outcrop (e.g., Fig. 2b,d,e,f). The importance of easily recognizable igneous components in the interpretation of such melt-transfer zones is highlighted by studies questioning the causal link between plutonism and faults or shear zones based on the lack of igneous components in the field (e.g., Paterson & Schmidt, 1999; Schmidt & Paterson, 2000).

Microstructures indicative for the former presence of melt

In general, migmatites (and igneous rocks) contain microstructures indicative the former presence of melt (Vernon, 2011 and references therein) including (1) minerals with well-defined crystal faces (Platten, 1982), (2) highly cuspate single grains with low dihedral angles interpreted to represent melt pseudomorphs (Sawyer, 2001; Holness, 2008; Walte et al., 2005), and (3) strings of beads of round blebs of pseudomorphed former melt (e.g., quartz) along grain boundaries (Holness, 2008). Specifically, rocks that deform in the presence of melt exhibit (a) euhedral felsic minerals in shear bands and elongate-cm scale pockets, and (b) presence of grains pseudomorphing melt films along grain boundaries and/or fractures (e.g., Daines & Kohlstedt, 1994; Sawyer, 1999; Rosenberg & Handy, 2000;

Rosenberg & Riller, 2000; Rosenberg & Berger, 2001; Marchildon & Brown, 2003; Walte et al., 2005; Holness, 2008; Schulmann et al., 2008; Vernon, 2011; Zavada et al., 2007, 2018). Reaction rims including symplectites may also form in response to the injection of external melt and its interaction with the host rock in both static and deforming rocks (Stuart et al., 2016, 2017; Daczko et al. 2016; Meek et al., 2019; Gardner et al., 2020; Silva et al., 2022).

High-strain zones with microstructures atypical of mylonite

We have recently recognized some ductile high-strain zones that have the general field appearance of solid-state high-strain deformation zones but lack typical mylonitic microstructures (Daczko et al. 2016; Stuart et al., 2018a,b; Meek et al., 2019; Piazolo et al., 2020; Gardner et al., 2020; Silva et al., 2022). Instead, they exhibit a set of distinct microstructures that include those commonly interpreted to be indicative of the former presence of melt, in contrast to the sub-solidus character of their melt-absent low-strain wall rocks.

In the field, these high-strain zones look like many mylonitic high-strain zones and exhibit a change in colour (Fig. 2a,c,f; Fig. 4c,d) due to changes to the mineral assemblage and/or reduction in grain size, compared to the wall rock. Additionally, they show deflections from the wall rock into the high-strain zone with a gradual change in fabric and foliation intensity and are strongly compositionally banded in shear zone centres (Fig. 4c,d). At the thin section scale, we observe microstructures unusual for mylonite. The most conspicuous microstructural feature is a general unimodal grain size distribution for each phase, compared to the common bimodal distributions associated with dynamic recrystallization commonly observed in mylonite (Figs. 1 & 3). Grains display limited internal deformation features (i.e., they lack or show very limited development of undulose extinction, deformation twins, subgrains, etc.), even if they are large grains expected to deform by dislocation creep. This contrasts with the large, crystal plastically deformed grains observed in mylonitic high strain rocks. Nevertheless, grains with high aspect ratios (e.g. biotite) may be strongly aligned (e.g., Fig. 4a_i,b_i,d_{ii}) so that grains or grain aggregates may define a shape-preferred orientation (Fig. 4c,d,d_i). Relict grains (porphyroclasts) may be observed in the transition between the high-strain zone and surrounding rocks but are rare within the high-strain zone (only a few grains can be noted on Fig. 4c_i,c_{ii},c_{iii}), somewhat similar to the transition seen from mylonite to ultramylonite. Micro-folding and asymmetric microstructures are less common than in typical mylonitic rocks (Fig. 4); although, it should be noted that some mylonite rocks may lack asymmetric structures.

Euhedral or partially faceted grains are common for one or two minerals within an assemblage (e.g., K-feldspar in Fig. 4a_{ii}; garnet in Fig. 4b_{iii}). The faceted grains are in contact with other minerals that may form elongate (aspect ratios >10) single grains (Fig. 4a_{ii},a_{iii},a_{iv},b_{iii},c_{iv},d_{iv}) or small (≤ 60°) dihedral angles at the junction of the faceted grains (Fig. 4a_{v},b_{iii},c_{iv},c_{v},d_{iii},d_{iv}). Note that careful observation is needed to distinguish a faceted grain boundary from gently curved grain boundaries in polygonal textures. Typically, within a neighbourhood of 10–20 grains, several of these xenomorphic grains show the same crystallographic orientation (i.e., same extinction angle, same interference colour), even though they are not connected in two dimensions, suggesting a single grain that branches in 3D (e.g., plagioclase in Fig. 4a_{iii} or quartz in Fig. 4b_{ii}). Fine grained, intergrown multiphase aggregates (e.g., quartz–plagioclase–K-feldspar) include the mineral(s) that form the interstitial textures (Fig. 4c_{v},d_{iii},d_{iv}). These are concave-shaped and observed at triple junctions, along grain boundaries and as mineral inclusions in the euhedral or partially facetted grains. Strings of rounded bleb-shaped minerals along grain boundaries (‘string of beads’ textures) are common (Holness et al., 2011; Lee et al., 2018), though, these can also be observed in mylonite at the start of forming a mortar texture. The ambiguity in some microstructures highlights the need to evaluate the full range of microstructures present.

Some high-strain zones that cut sub-solidus rocks that we have studied exhibit enrichment in biotite (Fig. 4a,b; Piazolo et al., 2020, Ghatak et al. 2022; Silva et al., 2022) or amphibole content (Fig. 4d; Stuart et al., 2018b). In the biotite-rich examples, felsic components in the high-strain zone form K-feldspar-plagioclase-quartz-rich lenses of varying thickness (< 5 cm; Fig. 4a). The minerals within the lenses are not internally deformed at both the outcrop and thin section scales (Fig. 4a inset; Fig. 4a_{ii},a_{iii}). K-feldspar crystals may form felsic lenses with quartz (Fig. 4a inset) or isolated grains (Fig. 4b inset). Biotite-rich selvedges (Fig. 4a) and anastomosing bands (Fig. 4b) may also contain small proportions of muscovite, sillimanite, magnetite and/or garnet. Fine cuspate grains of quartz and feldspar occur between biotite and garnet grains (Fig. 4a_{iii},b_{ii},b_{iii}). Reaction textures (Fig. 4b_{iv},b_{v}) may be common, where pre-existing grains (e.g., Grt, garnet, in b_{iv} and b_v, and Cpx, clinopyroxene, in c_{ii}) are partially replaced at grain margins and along dissolution channels and/or fractures (Fig. 4_{iv},b_v). A new feature noticed in preparing this review and synthesis of microstructures is that the pre-existing grains may be decorated with many fine-scale trails of porosity (e.g., trails of very fine circular features that are black in BSE and best observed in the garnet in Fig. 4b_{iv},b_v) or tiny inclusions (shown in the inset of Fig. 4b_v; grey in BSE), consistent with former fluid-filled porosity, a key indicator of fluid-mediated coupled dissolution-precipitation (e.g., Putnis et al., 2009; Varga et al., 2020; Halpin et al., 2020). An important point is that all the delicate microstructures highlighted on Figure 4 are very rare or absent in classic mylonite.

Discussion

High-strain zones with microstructures indicative of the former presence of melt but lacking high proportions of igneous material: characteristics and mechanisms

High-strain zones that display high proportions (>10%) of felsic or leucocratic material in outcrop, where the leucocratic material lacks internal sub-solidus deformation microstructures, are distinguished from migmatite subsequently deformed under sub-solidus conditions by the field geologist and therefore recognised as having experienced melt-present deformation. Such zones are reported from areas of regional supra-solidus migmatite domains containing overall high leucosome content (e.g., Brown & Solar, 1998a). However, few such high-strain zones are reported to occur in sub-solidus host rocks where the high-strain zone contains low proportions of felsic or leucocratic material (e.g., Daczko et al., 2016; Carvalho et al., 2016, 2017; Stuart et al., 2018a,b; Meek et al., 2019; Piazolo et al., 2020; Lee et al., 2020; Ghatak et al., 2022; Silva et al. 2022). Is this because they are truly rare, or perhaps they are under-recognised? Based on the combination of microstructural features, we interpret the high-strain zones described above as having formed during melt-present deformation in melt migration pathways through sub-solidus rocks, even though their outcrop pattern is largely compatible with mylonite deformed at sub-solidus conditions. This interpretation is based on five main sets of observations: these rocks 1) exhibit microstructures that are indicative of the former presence of melt and inferred to be associated with crystallisation of the final proportions of melt (in-situ or injected) in igneous rocks and migmatite (Sawyer, 1999; Holness, 2008; Vernon, 2011), 2) lack many of the microstructural features common to mylonite, 3) lack indications of later annealing within the high-strain zone and adjacent rocks, 4) are commonly too coarse grained to be interpreted as deforming by diffusion creep, and 5) contain abundant reaction replacement microstructures suggestive of open system melt-rock interaction during melt migration through the high-strain zones.

In equilibrated rocks with low proportions of melt (a few volume percent), the melt–solid dihedral angles control melt connectivity, such that the melt forms an interconnected grain boundary network of channels along three-grain junctions if the dihedral angle is less than 60° (Holness et al. 2011). Additionally, isolated pockets of melt may form on four-grain junctions if the melt–solid dihedral angle is greater than 60° or if the melt proportion in the rock is higher. The faceted grain boundaries observed in our high-strain rocks (e.g., K-feldspar in Fig. 4a$_{\mathrm{ii}}$ and garnet in 4b$_{\mathrm{iii}}$), where the system is interpreted to have been chemically open and reaction textures suggest it was in chemical disequilibrium (e.g., Fig. 4b$_{\mathrm{iv}}$, c$_{\mathrm{ii}}$), are inferred to have crystallised against melt in one of these melt-filled porosity scenarios. This results in the observed interstitial texture, including xenomorphic grains forming elongate single grains and those with small (≤ 60°) dihedral angles (Fig. 4; Holness, 2008 and references therein). As these xenomorphic grains pseudomorph the melt-filled network, some grains pseudomorph melt by forming an ‘overgrowth’ on an existing framework grain. These overgrowths may grow in a branching 3D structure between the other nearby solid minerals (fig. 3c in Holness et al., 2011). In this scenario, these pseudomorphs of melt form very irregularly-shaped, interstitial, single grains that intersect a 2D section in several places (Fig. 4a$_{\mathrm{iii}}$,b$_{\mathrm{ii}}$). During crystallisation, the very last melt proportions in a rock become isolated and hence trapped along grain boundaries and at three- or four-grain junctions (Sawyer, 1999; Vernon, 2011; Holness et al., 2011). These small pockets of isolated melt rarely crystallise into fine-grained, multiphase aggregates or “nanogranites” (Fig. 4d$_{\mathrm{iv}}$; Holness & Sawyer, 2008; Cesare et al., 2009). Reaction of an externally derived hydrous melt (and/or in rare cases the last melt trapped) results in local hydration reaction textures, where water is sourced from the melt (Fig. 4a,b; e.g., White & Powell, 2010; Carvalho et al., 2016; Stuart et al., 2016; Meek et al., 2019; Gardner et al., 2020; Piazolo et al., 2020; Ghatak et al., 2022). The melt-rock reaction may result in significant changes to whole rock major and minor element compositions at the large scale (Stuart et al., 2018b; Meek et al., 2019, Silva et al. 2022; Ghatak et al. 2022).

The common microstructures observed in typical mylonite form in response to differential stress at subsolidus conditions (e.g., White, 1979; Hobbs et al., 1986) and some of these are also observed in the high-strain zones described here. Therefore, the correct interpretation of the microstructure of a given high-strain rock relies on the weight of evidence for or against solid-state versus melt-present deformation. In mylonitic rocks deformed at solid-state conditions, the deformation processes involve crystal-plastic deformation and/or deformation by mass transfer. Further, for some minerals, contemporaneous brittle failure of grains may occur, forming the array of common microstructures in mylonite (Fig. 3 and Fig. 5). In contrast, stresses are largely dissipated through melt flow during melt-present deformation, thus decreasing the effective stress on the solid minerals and reducing the necessity of crystal-plastic deformation of grains. This is best recognised in magmatic flow (Nicolas et al., 1988; Paterson et al., 1998; Vernon, 2000), but in high stress situations of low melt volumes, it is unknown at what point the melt may not be able to accommodate deformation, thus activating other deformation processes. Consequently, at the grain scale, we expect to observe less crystal-plastic deformation features in high-strain rocks that formed during melt-present deformation. However, a shape- and/or crystallographic-preferred orientation may develop in melt-present high-strain zones due to rigid body rotation of the solid, elongate crystals (e.g., March, 1932; Jeffrey, 1922; Ghosh & Ramberg, 1976; Ildefonse et al., 1992; Ildefonse & Mancktelow, 1993; Arbaret et al., 1996; Piazolo & Passchier, 2002) and/or crystal growth within a stress field (e.g., Vernon, 1987). The preservation of the delicate microstructures observed in the studied examples (Fig. 4) suggests that little solid-state deformation occurred after the melt-present deformation. Hence, once these high-strain rocks cooled below the solidus or the proportion of melt decreased, they became rheologically strong and deformation stopped or was partitioned elsewhere (Carvalho et al., 2016, 2017; Stuart et al., 2018a,b; Prakash et al., 2018; Lee et al., 2018, 2020; Shao et al., 2021).

We now focus on the mechanism involved in the origin of the cryptic nature of syn-deformational melt-transfer zones through sub-solidus rocks. The microstructural features typical for melt present high-strain zones, as summarized in Figure 5, suggest that these zones develop by deformation-assisted porous melt flow (e.g., Meek et al., 2019). During porous melt flow (e.g., Kelemen et al., 1995), melt dominantly migrates along grain boundaries, hence microstructures pseudomorphing melt are preserved as grain boundary films with low dihedral angles, string of beads microstructures and three-dimensional grain networks. Such porous melt flow is possible if either there is a pre-existing network of melt along grain boundaries (case A) or if melt migration occurs in areas of high strain in sub-solidus rocks (case B). In Case A, the host rock is above its solidus with a small percent of melt present along grain boundaries forming an irregular melt network that can be exploited by the fluxing, externally derived melt (e.g., Stuart et al., 2016). Simultaneous deformation results in strain localisation and a local increase in the porosity and permeability of the high-strain zone (e.g., Edmond and Paterson, 1972, Fischer and Paterson, 1989; Katz et al., 2006; Hasalova et al., 2008, Schulmann et al., 2008; Stuart et al., 2018b) which lowers fluid pressure and creates sinks that draw melt towards zones of maximum deformation rate (Etheridge et al., 2021). In this scenario, dynamic opening and closing of pores in deforming rocks will continuously change local fluid pressure gradients resulting in a fluid pump (Fusseis et al., 2009; Menegon et al., 2015). The dynamic pressure changes are mainly facilitated by grain boundary sliding where melt films along grain boundaries enable sliding and geometric incompatibilities are accommodated dominantly by melt migration (e.g., Stuart et al., 2018b; Gardner et al., 2020). Consequently, a positive feedback loop develops where the high-strain zone becomes extremely weak, further focusing deformation. Melt accommodated grain boundary sliding is in stark contrast to grain boundary sliding in the solid state where either diffusion or dislocation glide are the dominant accommodating processes (e.g., Hirth and Kohlstedt, 2003; Svahnberg and Piazolo, 2010; Hansen et al., 2011). In case B, localised deformation in, for example, pre-existing fine grained host rocks may occur by grain boundary sliding (e.g., Fusseis et al., 2009). If grain boundary sliding occurs without accommodation by diffusion or dislocation glide, fluid (e.g., melt) will be drawn into the dynamic porosity associated with grain boundary sliding.

Microstructures in the host rock will be distinct for the two cases. In case A, the host rocks are expected to exhibit microstructures typical for low melt proportions, including asymmetric reaction microstructures. In contrast, in case B, the host rock is not expected to show any microstructures indicative of the former presence of melt. Here, field relationships would be consistent with syn-deformational melt migration of an externally derived melt through shear zones cutting solid rocks. In both cases, the concepts of deformation assisted melt flow through shear zones provides an effective mechanism to transport large volumes of melt through small volumes of rock (Stuart et al., 2018b; Silva et al., 2022). Accordingly, even though a large volume of melt may have migrated through such a high-strain zone, the frozen microstructural signatures of the former presence of melt are expected to be cryptic, i.e., visible at the thin section scale but not necessarily obvious at the outcrop scale. However, if melt flux is associated with extensive melt-rock interaction, microstructures indicative of the former presence of melt may still be cryptic, but geochemical signatures may be obvious both at the micro- and macroscale (e.g., Daczko et al. 2016, Stuart et al., 2018b; Meek et al., 2019; Silva et al., 2022). In this case, the deformation-assisted porous melt flow is highly reactive resulting in reaction front instabilities (e.g., Stuart et al., 2017; Meek et al., 2019) which may be enhanced by local deformation.

In summary, our review shows that rocks formed in melt-present high-strain zones do not always exhibit a high proportion of felsic or leucocratic material in outcrop when either small proportions of melt were only ever in the high-strain zone at one time or when subsequent melt loss occurs. Such high-strain zones are particularly cryptic when they form high-strain melt-migration pathways through sub-solidus rocks and can be easily overlooked and conflated with common solid-state mylonite. The mechanisms of deformation assisted porous melt flow results in the characteristics typical for such high-strain zones (Fig. 5).

Importance of recognising melt-present high-strain zones

Melt segregation, extraction and transfer through sub-solidus rocks: the type of heat source is the principal rate control on partial melting of the crust while deformation enables melt segregation and extraction (Brown, 1994, 2013; Sawyer, 1994; Etheridge et al., 2021). Melt segregation from a source initially involves grain boundary porous flow to sites of dilation on a similar time scale to partial melting (Rutter & Neuman, 1995; Brown, 2013 and references therein), while buoyancy of liquid relative to solid components, in combination with gravity- or deformation-driven compaction facilitates melt extraction (McKenzie, 1984; Rutter, 1997), possibly following accumulation in crustal settings (Diener et al., 2014). This must be an important process in the crust; for example, Brown (2008) suggests that up to 90% of crustal melt is extracted from its source.

While melt segregation and extraction in the anatectic zone are relatively well studied, less is known about melt transfer to the upper crust, especially through sub-solidus rocks. The current paradigm invokes two main mechanisms for melt transfer through the crust: flow in (1) dykes/hydrofractures or (2) shear zones (Guineberteau et al., 1987; Hutton, 1988; Hutton et al., 1990; Clemens & Mawer, 1992; McCaffrey, 1992; Mogk, 1992; Tikoff & Teyssier, 1992; Ingram & Hutton, 1994; Grocott et al., 1994, 2009; Collins & Sawyer, 1996; Brown & Rushmer, 1997; Brown & Solar, 1998b; Weinberg & Searle, 1998; Benn et al., 1999; Grocott & Taylor, 2002; Rosenburg, 2004; Richards & Collins, 2004; Denèle et al., 2008; Hasalová et al., 2008, 2011; Kisters et al, 2009; Sawyer, 2010; Vernon et al., 2012; Reichardt & Weinberg, 2012; Brown, 2013; Yakymchuk et al., 2013; Diener et al., 2014; Hall & Kisters, 2016; Daczko et al., 2016; Cavalho et al., 2016; Stuart et al., 2018a,b; Lee et al., 2018; Meek et al., 2019; Piazolo et al., 2020; Gardner et al., 2020; Etheridge et al., 2021; Silva et al., 2022; Ghatak et al., 2022). Granite (sensu lato) may be observed in shear bands and high-strain zones (Ashworth, 1976; Barr, 1985; Weinberg & Mark, 2008 and references therein; Hasalova et al., 2011; Carvalho et al., 2016). These relationships advocate for an effective role for ductile high-strain zones in magma ascent through the crust, where potentially large volumes of melt may move rapidly through a relatively narrow zone of rock that is heated by magmatic advection of heat during shearing (e.g., Cavalho et al., 2017).

Although a very challenging task, Stuart et al. (2018b) calculated minimum volumes of melt flux through amphibole-rich high-strain zones in the lower crust of magmatic arcs ranging between 0.26 and 2.0 m^3 of melt per m^3 of rock depending on the initial water content of the fluxing melt and the melt flux styles documented. Similarly, Silva et al. (2022) calculated minimum melt flux volumes through biotite-rich shear zones of Central Australia ranging between 0.03 to 0.23 m^3 of melt per m^3 of rock. When integrated over typical shear zone and crustal thicknesses, these volumes indicate migration of significant volumes of melt can occur through high-strain zones.

The composition of melt migrating through high-strain zones varies widely, being documented from felsic, such as in Central Australia (e.g., Piazolo et al., 2020; Silva et al., 2022; Ghatak et al., 2022) to mafic, such as in Fiordland, New Zealand (e.g., Daczko et al., 2016; Stuart et al., 2016, 2017, 2018a,b; Meek et al., 2019) and at mid-ocean ridge core complexes (Gardner et al., 2020; Zhang et al., 2020, 2021; Ghatak et al., 2022). Petrological and geochemical patterns in high-strain melt-migration pathways are complex and nearly unique to each study site and even in comparing samples from a single pathway (e.g., Stuart et al., 2018b). This is due to the highly variable geochemical outcomes of melt-rock interaction that are controlled by variability in (i) the composition of the melt source, (ii) extent of geochemical modification of the melt during reactive flow due to things like armouring, (iii) variation in rock types interacted with along melt migration pathways, and (iv) possible trapping of early crystallised minerals (i.e., phenocrysts in the migrating melts) during the collapse of pathways as melt supply is reduced. For these reasons, generalisations about petrological and geochemical constraints on melt transfer processes are difficult to make. However, petrological and geochemical information is highly useful in individual case studies of melt-transfer zones.

We suggest that high-strain melt-migration pathways might be under-recognised, particularly through sub-solidus low-strain wall rocks, and advocate for the careful microstructural assessment of each high-strain zone on a case-by-case basis.

Rheology: The presence of melt in deforming high-strain zones is thought to have a very significant rheological effect, where the zones weaken significantly by the physical presence of melt (e.g., Arzi, 1978; Rosenberg & Handy, 2005), even at low proportions of melt. The volume of melt and character of its distribution is a key control on the rheological behaviour of a melt-solid crystal system. Once the melt is interconnected along grain boundaries, the rheology of the rock will be very significantly weakened. The degree of weakening depends on the composition of the melt as the melt can interconnect along grain boundaries if the melt-solid dihedral angle is less than 60° (Holness, 2006, Holness et al., 2011) and the grain size, i.e., the boundary network length that needs wetting. Within a felsic system, Dell'Angelo and Tullis (1988) conclude that 2% melt is required for wetting grain boundaries and approximately 7% melt is required for full interconnectivity resulting in 1-2 orders of magnitude rheological weakening as strain is primarily accommodated by the melt (Bruhn et al. 2000; Rosenberg & Handy, 2005). The suggested weakening effect stems from the low viscosity of the melt relative to the solid framework of the crystalline rock. Other processes that may take place simultaneously and further enhance rheological weakening include grain size reduction (Arzi, 1978; Dell'Angelo & Tullis, 1988; Davidson et al., 1994; Rutter & Neumann, 1995; Mecklenburg & Rutter, 2003; van der Molen & Paterson, 1979; Paterson et al., 1998; Jamieson et al., 2011) and growth of rheologically “soft” minerals during melt-rock interaction, such as biotite (Rutter & Brodie, 1985; White & Powell, 2010; Piazolo et al., 2020; Silva et al., 2022) and sillimanite (Vernon, 2011). Reaction softening because of fluid-rock interaction between the host rock and the migrating fluid occurring in high-strain zones has been commonly inferred to have a positive feedback effect enhancing rheological weakening in high-strain zones and hence strain localization (e.g., Rubie, 1983; Rutter & Brodie, 1985). In addition, the presence of fluid pressure originating from either aqueous fluid or melt within an actively deforming high-strain zone may enhance rheological weakening (Hubbert & Rubey, 1959).

High-strain melt-migration pathways through sub-solidus rocks

The review and synthesis of microstructures presented here (Fig. 4) is inconsistent with the current usage of ‘mylonite’. In our view, it is a misnomer to call the studied high-strain rocks ‘mylonite’. Rocks that formed during melt-migration through high-strain zones that cut sub-solidus rocks and preserve low proportions of melt are rarely recognised. The above discussion highlights the potential importance of melt-present high-strain zones in terms of melt migration through sub-solidus rocks and for rheology of the crust. Consequently, it is imperative to distinguish between mylonite and high-strain melt-migration pathways through sub-solidus rocks. We suggest that a new term for crystalline rocks (in contrast to pseudotachyllite) produced in melt-present high-strain zones that cut sub-solidus rocks will assist in clarity of description and interpretation. We propose the term *melferite*, from the Greek *meldein*, "melt", and Latin *fer*, "that which carries", for rocks produced in high-strain melt-migration pathways though sub-solidus rocks and are currently conflated with genuine mylonite. We propose that geologists may choose call a rock ‘melferite’ like cataclasite (formed by cataclasis), or mylonite (formed by mylonitisation), etc. The distinguishing features of mylonite versus melferite are summarised in Figure 5. We hope that this research will encourage geologists to assess each high-strain zone on a case-by-case basis, in the light of solid-state versus melt-present deformation, particularly where the low-strain wall rocks are sub-solidus.

Acknowledgements

ARC Future Fellowship (FT110100070) & Discovery Project funding (DP120102060; DP160103449; DP200100482) provided financial support to conduct this research. Cait Stuart, Uvana Meek, David Silva, Hindol Ghatak, Robyn Gardner and Kim Jessop are thanked for the provision of field and thin section photos & discussions on melt-present deformation. We thank Luca Menegon for editorial handling & are grateful for insightful & constructive reviews by Luiz Morales & two anonymous reviewers. This is contribution XXX from the ARC Centre of Excellence for Core to Crust Fluid Systems (www.ccfs.mq.edu.au) & XXXX from the GEMOC Key Centre (www.gemoc.mq.edu.au).

References

Aldanmaz, E.R.C.A.N., Köprübaşı, N., Gürer, Ö.F., Kaymakçı, N., Gourgaud, A., 2006. Geochemical constraints on the Cenozoic, OIB-type alkaline volcanic rocks of NW Turkey: implications for mantle sources and melting processes. Lithos 86, 50–76.

Arbaret, L., Diot, H., Bouchez, J.L., 1996. Shape fabrics of particles in low concentration suspensions: 2D analogue experiments and application to tiling in magma. Journal of Structural Geology 18, 941–950.

Arzi, A.A., 1978. Critical phenomena in the rheology of partially melted rocks. Tectonophysics 44, 173-184.

Ashworth, J.R., 1976. Petrogenesis of migmatites in the Huntly-Portsoy area, north-east Scotland. Mineralogical Magazine 40, 661–682.

Bailey, C.M., Polvi, L.E., Forte, A.M., 2007. Pure shear dominated high-strain zones in basement terranes. Memoirs, Geological Society of America 200, 93.

Barr, D., 1985. Migmatites in the Moines. In Migmatites (pp. 225–264). Springer, Boston, MA.

Bell, T.H., Etheridge, M.A., 1973. Microstructure of mylonites and their descriptive terminology. Lithos 6, 337–348.

Benn, K., Roest, W.R., Rochette, P., Evans, N.G., Pignotta, G.S., 1999. Geophysical and structural signatures of syntectonic batholith construction: the South Mountain Batholith, Meguma Terrane, Nova Scotia. Geophys. J. Int. 136, 144–158.

Bhattacharya, S., Kemp, A.I.S., Collins, W.J., 2018. Response of zircon to melting and metamorphism in deep arc crust, Fiordland (New Zealand): implications for zircon inheritance in cordilleran granites. Contributions to Mineralogy and Petrology 173, 28.

Bons, P.D., Dougherty-Page, J., Elburg, M.A., 2001. Stepwise accumulation and ascent of magmas. Journal of Metamorphic Geology 19, 627–633.

Bose, S., Sengupta, S., 2003. High temperature mylonitization of quartzofeldspathic gneisses: Example from the Schirmacher Hills, East Antarctica. Gondwana Research 6, 805–816.

Bouchez, J.L., Delas, C., Gleizes, G., Nédélec, A., Cuney, M., 1992. Submagmatic microfractures in granites. Geology 20, 35–38.

Brown, M., 1973. The definition of metatexis, diatexis and migmatite. Proceedings of the Geologists' Association 84, 371–382.

Brown, M., 1994. The generation, segregation, ascent and emplacement of granite magma: the migmatite-to-crustally-derived granite connection in thickened orogens. Earth-Science Reviews 36, 83–130.

Brown, M., 2008. Granites, migmatites and residual granulites: relationships and processes. Working with migmatites. Edited by EW Sawyer and M. Brown. Mineralogical Association of Canada, Short Course Series 38, 97–144.
Brown, M., 2013. Granite: From genesis to emplacement. Geological Society of America Bulletin 125, 1079-1113.
Brown, M., Rushmer, T., 1997. The role of deformation in the movement of granitic melt: views from the laboratory and the field, in: Holness, M.B. (Ed.), Deformation-enhanced Fluid Transport in the Earth's Crust and Mantle. Springer, pp. 111–144.
Brown, M., Solar, G.S., 1998a. Shear-zone systems and melts: feedback relations and self-organization in orogenic belts. Journal of Structural Geology 20, 211–227.
Brown, M., Solar, G.S., 1998b. Granite ascent and emplacement during contractional deformation in convergent orogens. Journal of Structural Geology 20, 1365–1393.
Bruhn, D., Groebner, N., Kohlstedt, D.L., 2000. An interconnected network of core-forming melts produced by shear deformation. Nature 403, 883–886.
Carreras, J., Druguet, E., Griera, A., 2005. Shear zone-related folds. Journal of Structural Geology 27, 1229–1251.
Carvalho, B.B., Sawyer, E.W., Janasi, V.A., 2016. Crustal reworking in a shear zone: transformation of metagranite to migmatite. Journal of Metamorphic Geology 34, 237–264.
Carvalho, B.B., Janasi, V.A., Sawyer, E.W., 2017. Evidence for Paleoproterozoic anatexis and crustal reworking of Archean crust in the São Francisco Craton, Brazil: A dating and isotopic study of the Kinawa migmatite. Precambrian Research 291, 98–118.
Castro, A., 1986. Structural pattern and ascent model in the central Extramadura batholith, Hercynian belt, Spain. Journal of Structural Geoogy 8, 633–645.
Cesare, B., Ferrero, S., Salvioli-Mariani, E., Pedron, D., Cavallo, A., 2009. "Nanogranite" and glassy inclusions: The anatectic melt in migmatites and granulites. Geology 37, 627–630.
Christie, J.M., 1963. The Moine thrust zone in the Assynt region, northwest Scotland. University of California Press.
Clemens, J.D., 1998. Observations on the origins and ascent mechanisms of granitic magmas. Journal of the Geological Society 155, 843–851.
Clemens, J.D., Mawer, C.K., 1992. Granitic magma transport by fracture propagation. Tectonophysics 204, 339–360.
Collins, W.J., Sawyer, E.W., 1996. Pervasive granitoid magma transfer through the lower–middle crust during non-coaxial compressional deformation. Journal of Metamorphic Geology 14, 565–579.
Collins, W. J., Wiebe, R. A., Healy, B. & Richards, S. W. 2006. Replenishment, crystal accumulation and floor aggradation in the megacrystic Kameruka Suite, Australia, Journal of Petrology 47, 2073–104.
Craven, S.J., Daczko, N.R., Halpin, J.A., 2013. High-T–low-P thermal anomalies superposed on biotite-grade rocks, Wongwibinda Metamorphic Complex, southern New England Orogen, Australia: heat advection by aqueous fluid? Australian Journal of Earth Sciences 60, 621–635.
Cruden, A.R., Weinberg, R.F., 2018. Mechanisms of magma transport and storage in the lower and middle crust—magma segregation, ascent and emplacement. In Volcanic and Igneous Plumbing Systems (pp. 13–53). Elsevier.
Daczko, N.R., Klepeis, K.A., Clarke, G.L. 2001. Evidence of Early Cretaceous collisional-style orogenesis in northern Fiordland, New Zealand and its effects on the evolution of the lower crust. Journal of Structural Geology 23, 693–713.
Daczko, N.R., Klepeis, K.A., Clarke, G.L. 2002a. Thermo-mechanical evolution of the crust during convergence and deep crustal pluton emplacement in the western province of Fiordland, New Zealand. Tectonics 21, 1022.
Daczko, N.R., Stevenson, J.A., Clarke, G.L., Klepeis, K.A. 2002b. Successive hydration and dehydration of a high-P mafic granofels involving clinopyroxene-kyanite symplectites, Mt Daniel, Fiordland, New Zealand. Journal of Metamorphic Geology 20, 669–682.
Daczko, N.R., Emami, S., Allibone, A.H., Turnbull, I.M., 2012. Petrogenesis and geochemical characterisation of ultramafic cumulate rocks from Hawes Head, Fiordland, New Zealand. New Zealand Journal of Geology and Geophysics 55, 361–374.
Daczko, N.R., Piazolo, S., Meek, U., Stuart, C.A., Elliott, V., 2016. Hornblendite delineates zones of mass transfer through the lower crust. Scientific Reports 6, 31369.
Daines, M.J., Kohlstedt, D.L., 1994. The transition from porous to channelized flow due to melt/rock reaction during melt migration. Geophysical Research Letters 21, 145–148.

Davidson, C., Schmid, S.M., Hollister, L.S., 1994. Role of melt during deformation in the deep crust. Terra Nova 6, 133-142.

de Freitas, N.C., Almeida, J., Heilbron, M., Cutts, K., Dussin, I., 2021. The Cabo Frio Thrust: A folded suture zone, Ribeira belt, SE Brazil. Journal of Structural Geology 149, 104379.

de Saint Blanquat, M.,Tikoff, B.,Teyssier, C.,Vigneresse, J.L., 1998.Transpressional kinematics and magmatic arcs. Holdsworth, R.E., Strachan, R.A., Dewey, J.F. (Eds.), Continental Transpressional and Transtensional Tectonics. Special Publications 135, Geological Society, London, 327–340.

Dell'Angelo, L.N., Tullis, J., 1988. Experimental deformation of partially melted granitic aggregates. Journal of Metamorphic Geology 6, 495–515.

Denèle, Y., Olivier, P., Gleizes, G., 2008. Progressive deformation of a zone of magma transfer in a transpressional regime: The Variscan Mérens shear zone (Pyrenees, France). Journal of Structural Geology 30, 1138–1149.

Diener, J.F., White, R.W., Hudson, T.J., 2014. Melt production, redistribution and accumulation in mid-crustal source rocks, with implications for crustal-scale melt transfer. Lithos 200, 212–225.

Edmond, J.M., Paterson, M.S., 1972. Volume changes during the deformation of rocks at high pressures. International Journal of Rock Mechanics and Mining Science 9, 161–182.

Etheridge, M., Daczko, N.R., Chapman, T., Stuart, C.A., 2021. Mechanisms of melt extraction during lower crustal partial melting. Journal of Metamorphic Geology 39, 57–75.

Fischer, G.J., Paterson, M.S., 1989. Dilatancy during rock deformation at high temperatures and pressures. Journal of Geophysical Research 94, 607–617.

Fusseis, F., Regenauer-Lieb, K., Liu, J., Hough, R.M., De Carlo, F., 2009. Creep cavitation can establish a dynamic granular fluid pump in ductile shear zones. Nature 459, 974–977.

Gardner, R., Piazolo, S., Daczko, N.R., 2015. Pinch and swell structures: Evidence for strain localization by brittle-viscous behaviour in the middle crust. Solid Earth 6, 1045–1061.

Gardner, R., Piazolo, S., Daczko, N.R., Trimby, P., 2020. Microstructures reveal multistage melt present strain localisation in mid-ocean gabbros. Lithos 366, 105572.

Geshi, N., 2001. Melt segregation by localized shear deformation and fracturing during crystallization of magma in shallow intrusions of the Otoge volcanic complex, central Japan. Journal of Volcanology and Geothermal Research 106, 285–300.

Ghatak, H., Gardner, R., Daczko, N.R., Piazolo, S., Raimondo, T., 2022. Oxide enrichment by syntectonic melt-rock interaction. Lithos 414 (106617).

Ghosh, S.K., Ramberg, H., 1976. Reorientation of inclusions by combination of pure shear and simple shear. Tectonophysics 34, 1–70.

Gibson, G. M., McDougall, I., Ireland, T. R., 1988. Age constraints on metamorphism and the development of a metamorphic core complex in Fiordland, southern New Zealand. Geology 16, 405–408.

Grocott, J.,Taylor, G.K., 2002. Magmatic arc fault systems, deformation partitioning and emplacement of granitic complexes in the Coastal Cordillera, north Chilean Andes (25°30′S to 27°00′S). Journal of the Geological Society of London 159, 425–442.

Grocott, J., Brown, M., Dallmeyer, R.D.,Taylor, G.K.,Treloar, P.J., 1994. Mechanisms of continental growth in extensional arcs: an example from the Andean plate-boundary zone. Geology 22, 391–394.

Grocott, J.,Arevalo, C.,Welkner, D., Cruden,A.R., 2009. Fault-assisted vertical pluton growth: coastal Cordillera, northern Chilean Andes. Journal of the Geological Society of London 166, 295–301.

Guineberteau, B., Bouchez, J.L.,Vigneresse, J.L., 1987.The Mortagne granite pluton (France) emplaced by pull-apart along a shear zone: structural and gravimetric arguments and regional implications. Geological Society of America Bulletin 99, 763–770.

Hall, D., Kisters, A., 2016. Episodic granite accumulation and extraction from the mid-crust. Journal of Metamorphic Geology 34, 483–500.

Halpin, J.A., Daczko, N.R., Direen, N.G., Mulder, J.A., Murphy, R.C., Ishihara, T., 2020. Provenance of rifted continental crust at the nexus of East Gondwana breakup. Lithos 354, 105363.

Hanmer, S., Passchier, C.W., 1991. Shear sense indicators: a review. Geological Survey of Canada Paper, 90, pp. 1–71.

Hansen, L.N., Zimmerman, M.E., Kohlstedt, D.L., 2011. Grain boundary sliding in San Carlos olivine: flow law parameters and crystallographic-preferred orientation. Journal of Geophysical Research, Solid Earth 116, B08201.

Hasalová, P., Stipská, P., Powell, R., Schulmann, K., Janouek, V., Lexa, O., 2008.Transforming mylonitic metagranite by open-system interactions during melt flow. Journal of Metamorphic Geology 26, 55–80.

Hasalová, P., Weinberg, R.F., Macrae, C., 2011. Microstructural evidence for magma confluence and reusage of magma pathways: implications for magma hybridization, Karakoram Shear Zone in NW India. Journal of Metamorphic Geology 29, 875-900.

Heilbronner, R., Tullis, J., 2002. The effect of static annealing on microstructures and crystallographic preferred orientations of quartzites experimentally deformed in axial compression and shear. Geological Society of London, Special Publication 200, 191–218.

Higgins, M. D. 1998. Origin of anorthosite by textural coarsening: Quantitative measurements of a natural sequence of textural development. Journal of Petrology 39, 1307–23.

Hippertt, J., Rocha, A., Lana, C., Egydio-Silva, M., Takeshita, T., 2001. Quartz plastic segregation and ribbon development in high-grade striped gneisses. Journal of Structural Geology 23, 67–80.

Hirth, G., Kohlstedt, D., 2003. Rheology of the upper mantle and the mantle wedge: a view from the experimentalists, inside the subduction factory. Geophysical monograph - American Geophysical Union 138, 83–106.

Hobbs, B.E., Means, W.D., Williams, P.F., 1976. An outline of structural geology. Wiley.

Hobbs, B.E., Ord, A., Teyssier, C., 1986. Earthquakes in the ductile regime? Pure and Applied Geophysics 124, 309–336.

Hollister, L.S., Crawford, M.L., 1986. Melt-enhanced deformation: A major tectonic process. Geology 14, 558–561.

Holness, M.B., Watt, G.R., 2002. The aureole of the Traigh Bhan na Sgurra sill, Isle of Mull: reaction-driven micro-cracking during pyrometamorphism. Journal of Petrology 43, 511-534.

Holness, M.B., Cheadle, M.J., McKenzie, D.A.N., 2005. On the use of changes in dihedral angle to decode late-stage textural evolution in cumulates. Journal of Petrology 46, 1565–1583.

Holness, M.B., 2008. Decoding migmatite microstructures, in: Sawyer, E.W., Brown, M. (Eds.), Working with Migmatites. Mineralogical Association of Canada, pp. 57–76.

Holness, M.B., Sawyer, E.W., 2008. On the pseudomorphing of melt-filled pores during the crystallization of migmatites. Journal of Petrology 49, 1343–1363.

Holness, M.B., Cesare, B., Sawyer, E.W., 2011. Melted rocks under the microscope: microstructures and their interpretation. Elements 7, 247–252.

Holness, M.B., Vernon, R.H., 2015. The influence of interfacial energies on igneous microstructures. In Layered intrusions (pp. 183–228). Springer, Dordrecht.

Hubbert, M.K., Rubey, W.W., 1959. Role of fluid pressure in mechanics of overthrust faulting I. Mechanics of fluid-filled porous solids and its application to overthrust faulting. Geological Society of America Bulletin 70, 115–166.

Hutton, D.H.W., 1988. Granite emplacement mechanisms and tectonic controls: inferences from deformation studies. Transactions of the Royal Society of Edinburgh 79, 245–255.

Hutton, D.H.W., Dempster, T.J., Brown, P.E., Becker, S.M., 1990. A new mechanism of granite emplacement: intrusion into active extensional shear zones. Nature 343, 452–455.

Ildefonse, B., Sokoutis, D., Mancktelow, N.S., 1992. Mechanical interactions between rigid particles in a deforming ductile matrix. Analogue experiments in simple shear flow. Journal of Structural Geology 14, 1253–1266.

Ildefonse, B., Mancktelow, N.S., 1993. Deformation around rigid particles: the influence of slip at the particle/matrix interface. Tectonophysics 221, 345–359.

Ingram, G.I., Hutton, D.H.W., 1994.The great Tonalite Sill: emplacement into a contractional shear zone and implications for Late Cretaceous to early Eocene tectonics in southeastern Alaska and British Columbia. Geological Society of America Bulletin 106, 715–728.

Jamieson, R.A., Unsworth, M.J., Harris, N.B., Rosenberg, C.L., Schulmann, K., 2011. Crustal melting and the flow of mountains. Elements 7, 253–260.

Jeffery, G. B. 1922. The motion of ellipsoidal particles immersed in a viscous fluid. *Proceedings of the Royal Society* A 102, 161–179.

Jessell, M.W., 1987. Grain-boundary migration microstructures in a naturally deformed quartzite. Journal of Structural Geology 9, 1007–1014.

Jessop, K., Daczko, N.R., Piazolo, S., 2020. Two belts of HTLP sub-regional metamorphism in the New England Orogen, eastern Australia: occurrence and characteristics exemplified by the Wongwibinda Metamorphic Complex. Australian Journal of Earth Sciences 67, 1–29

Jiang, D., Williams, P.F., 1998. High-strain zones: a unified model. Journal of Structural Geology 20, 1105–1120.

Johannes, W., Gupta, L.N., 1982. Origin and evolution of a migmatite. Contributions to Mineralogy and Petrology 79, 114–123.

Katz, R.F., Spiegelman, M., Holtzman, B., 2006. The dynamics of melt and shear localization in partially molten aggregates. Nature 442, 676–679.

Kelemen, P.B., Dick, H.J.B., Quick, J.E., 1992. Formation of harzburgite by pervasive melt/rock reaction in the upper mantle. Nature 358, 635–641.

Kisters, A.F.M., Ward, R.A., Anthonissen, C.J. and Vietze, M.E., 2009. Melt segregation and far-field melt transfer in the mid-crust. Journal of the Geological Society 166, 905–918.

Klepeis, K.A., Daczko, N.R., Clarke, G.L. 1999. Kinematic vorticity and tectonic significance of superposed mylonites in a major lower crustal shear zone, northern Fiordland, New Zealand. Journal of Structural Geology 21, 1385–1405.

Lapworth, C., 1885. The Highland controversy in British geology: its causes, course and consequences. Nature 32, 558–559.

Law, R.D., 1990. Crystallographic fabrics: a selective review of their applications to research in structural geology. Geological Society of London, Special Publications 54, 335–352.

Lee, A.L., Torvela, T., Lloyd, G.E., Walker, A.M., 2018. Melt organisation and strain partitioning in the lower crust. Journal of Structural Geology 113, 188–199.

Lee, A.L., Lloyd, G.E., Torvela, T., Walker, A.M., 2020. Evolution of a shear zone before, during and after melting. Journal of the Geological Society 177, 738–751.

Lister, G.S., Snoke, A.W., 1984. SC mylonites. Journal of Structural Geology 6, 617–638.

March, A., 1932. Mathematische Theorie der Regelung nach der Korngestah bei affiner Deformation. Zeitschrift für Kristallographie-Crystalline Materials 81, 285–297.

Marchildon, N., Brown, M., 2003. Spatial distribution of melt-bearing structures in anatectic rocks from Southern Brittany, France: implications for melt transfer at grain- to orogen-scale. Tectonophysics 364, 215-235.

McCaffrey, K.J.W., 1992. Igneous emplacement in a transpressive shear zone: Ox Mountains igneous complex. Journal of the Geological Society 149, 221–235.

McKenzie, D.A.N., 1984. The generation and compaction of partially molten rock. Journal of Petrology 25, 713–765.

Mecklenburgh, J., Rutter, E.H., 2003. On the rheology of partially molten synthetic granite. Journal of Structural Geology 25, 1575-1585.

Menegon, L., Fusseis, F., Stünitz, H., Xiao, X., 2015. Creep cavitation bands control porosity and fluid flow in lower crustal shear zones. Geology 43, 227–230.

Meek, U., Piazolo, S., Daczko, N.R., 2019. The field and microstructural signatures of deformation-assisted melt transfer: insights from magmatic arc lower crust, New Zealand. Journal of Metamorphic Geology 37, 795–821.

Menegon, L., Fusseis, F., Stünitz, H., Xiao, X., 2015. Creep cavitation bands control porosity and fluid flow in lower crustal shear zones. Geology 43, 227–230.

Miller, R.B., Paterson, S.R., 1994. The transition from magmatic to high-temperature solid-state deformation: implications from the Mount Stuart batholith, Washington. Journal of Structural Geology 16, 853–865.

Mogk, D.W., 1992. Ductile shearing and migmatization at midcrustal levels in an Archean high-grade gneiss belt, Northern Gallatin Range, Montana, USA. Journal of Metamorphic Geology 10, 427–438.

Mukherjee, S., 2017. Review on symmetric structures in ductile shear zones. International Journal of Earth Sciences 106, 1453–1468.

Nicolas, A., Reuber, I., Benn, K., 1988. A new magma chamber model based on structural studies in the Oman ophiolite. Tectonophysics 151, 87–105.

Park, A.F., 1983. Lit-par-lit migmatite fabrics in a metagabbroanorthosite complex, Sygnefjell, Jotunheimen, South Norway. Migmatites, melting and metamorphism, 296.

Passchier, C.W., Trouw, R.A.J., 2005. Microtectonics. Springer Berlin Heidelberg.

Paterson, S.R., Vernon, R.H., Tobisch, O.T., 1989. A review of criteria for the identification of magmatic and tectonic foliations in granitoids. Journal of Structural Geology 11, 349–363.

Paterson, S.R., Fowler Jr, T.K., Schmidt, K.L., Yoshinobu, A.S., Yuan, E.S., Miller, R.B., 1998. Interpreting magmatic fabric patterns in plutons. Lithos 44, 53–82.

Paterson, S.R., Schmidt, K.L., 1999. Is there a close spatial relationship between plutons and faults? Journal of Structural Geology 21, 1131–1142.

Paterson, S. R., Vernon, R. H. & Za´k, J. 2005. Mechanical instabilities and accumulations of K-feldspar megacrysts in granitic magma, Tuolumne Intrusive Suite, California, USA. In Ko¨hn D. (ed.) General Contributions 2005. Journal of the Virtual Explorer 18. Paper 1.

Petford, N., Lister, J.R., Kerr, R.C., 1994. The ascent of felsic magmas in dykes. Lithos 32, 161–168.
Piazolo, S. and Passchier, C.W., 2002. Controls on lineation development in low to medium grade shear zones: a study from the Cap de Creus peninsula, NE Spain. Journal of Structural Geology 24, 25–44.
Piazolo, S., Bons, P.D., Jessell, M.W., Evans, L., Passchier, C.W., 2002. Dominance of microstructural processes and their effect on microstructural development: insights from numerical modelling of dynamic recrystallization. Geological Society, London, Special Publications 200, 149–170.
Piazolo, S., Bestmann, M., Prior, D.J., Spiers, C.J., 2006. Temperature dependent grain boundary migration in deformed-then-annealed material: observations from experimentally deformed synthetic rocksalt. Tectonophysics 427, 55–71.
Piazolo, S., Daczko, N.R., Silva, D., Raimondo, T., 2020. Melt-present shear zones enable intracontinental orogenesis. Geology 48, 643–648.
Pitcher, W.S., 1979. The nature, ascent and emplacement of granitic magmas. Journal of the Geological Society of London 136, 627–662.
Platten, I.M., 1982. Partial melting of feldspathic quartzite around late Caledonian minor intrusions in Appin, Scotland. Geological Magazine 119, 413–419.
Poirier, J.P., 1980. Shear localization and shear instability in materials in the ductile field. Journal of Structural Geology 2, 135–142.
Prakash, A., Piazolo, S., Saha, L., Bhattacharya, A., Pal, D.K., Sarkar, S., 2018. Deformation behavior of migmatites: insights from microstructural analysis of a garnet–sillimanite–mullite–quartz–feldspar-bearing anatectic migmatite at Rampura–Agucha, Aravalli–Delhi Fold Belt, NW India. International Journal of Earth Sciences 107, 2265–2292.
Putnis, A., Oelkers, E.H., Schott, J., 2009. Mineral replacement reactions. Thermodynamics and kinetics of water-rock interaction 70, 87–124.
Ramsay, J.G., 1980. Shear zone geometry: a review. Journal of Structural Geology 2, 83–99.
Reichardt, H., Weinberg, R.F., 2012. The dike swarm of the Karakoram shear zone, Ladakh, NW India: linking granite source to batholith. Geological Society of America Bulletin 124, 89–103.
Richards, S.W., Collins, W.J., 2004. Growth of wedge-shaped plutons at the base of active half grabens. Transactions of the Royal Society of Edinburgh 95, 309–317.
Rosenberg, C.L., 2004. Shear zones and magma ascent: a model based on a review of the Tertiary magmatism in the Alps. Tectonics, 23.
Rosenberg, C.L., Berger, A., 2001. Syntectonic melt pathways in granitic gneisses, and melt-induced transitions in deformation mechanisms. Physics and Chemistry of the Earth, Part A: Solid Earth and Geodesy 26, 287–293.
Rosenberg, C.L., Handy, M.R., 2000. Syntectonic melt pathways during simple shearing of a partially molten rock analogue (Norcamphor-Benzamide). Journal of Geophysical Research: Solid Earth 105, 3135–3149.
Rosenberg, C.L., Handy, M.R., 2005. Experimental deformation of partially melted granite revisited: implications for the continental crust. Journal of Metamorphic Geology 23, 19–28.
Rosenberg, C.L., Riller, U., 2000. Partial-melt topology in statically and dynamically recrystallized granite. Geology 28, 7–10.
Rubie, D.C., 1983. Reaction-enhanced ductility: The role of solid-solid univariant reactions in deformation of the crust and mantle. Tectonophysics 96, 331–352.
Rubin, A.M., 1995. Propagation of magma-filled cracks. Annual Review of Earth and Planetary Science 23, 287–336.
Rutter, E.H., 1997. The influence of deformation on the extraction of crustal melts: a consideration of the role of melt-assisted granular flow. Mineralogical Society Series 8, 82–110.
Rutter, E.H., Brodie, K.H., 1985. The permeation of water into hydrating shear zones. In Metamorphic Reactions (pp. 242–250). Springer, New York, NY.
Rutter, E.H., Neumann, D.H.K., 1995. Experimental deformation of partially molten Westerly granite under fluid-absent conditions, with implications for the extraction of granitic magmas. Journal of Geophysical Research: Solid Earth 100(B8), 15697–15715.
Sander, B., 1912. Ueber einige Gesteinsarten des Tauernwestendes. Jahrbuch der kaiserlichen koeniglichen geologischen Reichsanstalt 62, 219–288.
Sawyer, E.W., 1994. Melt segregation in the continental crust. Geology 22, 1019–1022.
Sawyer, E.W., 1999. Criteria for the recognition of partial melting. Physics and Chemistry of the Earth, Part A: Solid Earth and Geodesy 24, 269–279.

Sawyer, E.W., 2001. Melt segregation in the continental crust: distribution and movement of melt in anatectic rocks. Journal of Metamorphic Geology 19, 291–309.

Sawyer, E.W., 2010. Migmatites formed by water-fluxed partial melting of a leucogranodiorite protolith: microstructures in the residual rocks and source of the fluid. Lithos 116, 273–286.

Schulmann, K., Martelat, J.-E., Ulrich, S., Lexa, O., Štípská, P., Becker, J.K., 2008. Evolution of microstructure and melt topology in partially molten granitic mylonite: Implications for rheology of felsic middle crust. Journal of Geophysical Research: Solid Earth 113.

Schmidt, K.L., Paterson, S.R., 2000. Analyses fail to find coupling between deformation and magmatism, Eos 81, 197, 202–203.

Scott, D.R., Stevenson, D.J., 1986. Magma ascent by porous flow. Journal of Geophysical Research: Solid Earth 91(B9), 9283–9296.

Shao, Y., Piazolo, S., Liu, Y., Lee, A.L., Jin, W., Li, W., Liang, C., Wen, Q., 2021. Deformation Behavior and Inferred Seismic Properties of Tonalitic Migmatites at the Time of Pre-melting, Partial Melting, and Post-Solidification. Geochemistry, Geophysics, Geosystems 22, e2020GC009202.

Silva, D., Daczko, N. R., Piazolo, S., Raimondo, T., 2022. Glimmerite: a product of melt-rock interaction within a crustal-scale high strain zone. Gondwana Research 105, 160–184.

Simpson, C., De Paor, D.G., 1993. Strain and kinematic analysis in general shear zones. Journal of Structural Geology 15, 1–20.

Sleep, N.H., 1974. Segregation of magma from a mostly crystalline mush. Geological Society of America Bulletin 85(8), 1225–1232.

Stipp, M., StuÈnitz, H., Heilbronner, R., Schmid, S.M., 2002. The eastern Tonale fault zone: a 'natural laboratory' for crystal plastic deformation of quartz over a temperature range from 250 to 700 C. Journal of Structural Geology 24, 1861–1884.

Stokes, M.R., Wintsch, R.P., Southworth, C.S., 2012. Deformation of amphibolites via dissolution–precipitation creep in the middle and lower crust. Journal of Metamorphic Geology 30, 723–737.

Stuart, C.A., Piazolo, S., Daczko, N.R., 2016. Mass transfer in the lower crust: Evidence for incipient melt assisted flow along grain boundaries in the deep arc granulites of Fiordland, New Zealand. Geochemistry, Geophysics, Geosystems 17, 3733–3753.

Stuart, C.A., Daczko, N.R., Piazolo, S., 2017. Local partial melting of the lower crust triggered by hydration through melt–rock interaction: an example from Fiordland, New Zealand. Journal of Metamorphic Geology 35, 213–230.

Stuart, C.A., Piazolo, S., Daczko, N.R., 2018a. The recognition of former melt flux through high-strain zones. Journal of Metamorphic Geology 36, 1049–1069.

Stuart, C.A., Meek, U., Daczko, N.R., Piazolo, S., Huang, J.-X., 2018b. Chemical signatures of melt–rock interaction in the root of a magmatic arc. Journal of Petrology 59, 321–340.

Svahnberg, H., Piazolo, S., 2010. The initiation of strain localisation in plagioclase-rich rocks: Insights from detailed microstructural analyses. Journal of Structural Geology 32, 1404–1416.

Tanton, L.T.E., Grove, T.L., Donnelly-Nolan, J. 2001. Hot, shallow mantle melting under the Cascades volcanic arc. Geology 29, 631–634.

Tikoff, B.,Teyssier, C., 1992. Crustal-scale, en-echelon "P-shear" tensional bridges: A possible solution to the batholithic room problem. Geology 20, 927–930.

Tommasi, A., Vauchez, A., Femandes, L.A.D., Porcher, C.C., 1994. Magma-assisted strain localization in an orogen-parallel transcurrent shear zone of southern Brazil. Tectonics 13, 421–437.

Tullis, J., Snoke, A.W., Todd, V.R., 1982. Significance and petrogenesis of mylonitic rocks. Geology 10, 227–230.

van der Molen, I., Paterson, M.S., 1979. Experimental deformation of partially-melted granite. Contributions to Mineralogy and Petrology 70, 299–318.

Varga, J., Raimondo, T., Daczko, N.R., Adam, J., 2020. Experimental alteration of monazite in granitic melt: Variable U–Th–Pb and REE mobility during melt-mediated coupled dissolution-precipitation. Chemical Geology 544, 119602.

Vernon, R. H. 1986. K-feldspar megacrysts in granites – phenocrysts, not porphyroblasts. Earth-Science Reviews 23, 1–63.

Vernon, R.H., 1987. Oriented growth of sillimanite in andalusite, Placitas–Juan Tabo area, New Mexico, USA. Canadian Journal of Earth Sciences 24, 580–590.

Vernon, R. H. 2000. Review of microstructural evidence of magmatic and solid-state flow. Electronic Geosciences 5:2.

Vernon, R. H. 2004. A practical guide to rock microstructure. Cambridge: Cambridge University Press.

Vernon, R.H., 2011. Microstructures of melt-bearing regional metamorphic rocks. Geological Society of America Memoirs 207, 1–11.
Vernon, R.H., Paterson, S.R., 2006. Mesoscopic structures resulting from crystal accumulation and melt movement in granites. Earth and Environmental Science Transactions of the Royal Society of Edinburgh 97, 369–381.
Vernon, R.H., Collins, W.J., Cook, N.D.J., 2012. Metamorphism and deformation of mafic and felsic rocks in a magma transfer zone, Stewart Island, New Zealand. Journal of Metamorphic Geology 30, 473–488.
Vigneresse, J.L., 1995. Control of granite emplacement by regional deformation. Tectonophysics 249, 173–186.
Walte, N.P., Bons, P.D., Passchier, C.W., 2005. Deformation of melt-bearing systems—insight from in situ grain-scale analogue experiments. Journal of Structural Geology 27, 1666–1679.
Weinberg, R.F., Searle, M.P., 1998. The Pangong Injection Complex, Indian Karakoram: a case of pervasive granite flowthrough hot viscous crust. Journal of the Geological Society 155, 883–891.
Weinberg, R.F., Mark, G., 2008. Magma migration, folding, and disaggregation of migmatites in the Karakoram Shear Zone, Ladakh, NW India. Geological Society of America Bulletin 120, 994–1009.
White, S., 1979. Grain and sub-grain size variations across a mylonite zone. Contributions to Mineralogy and Petrology 70, 193–202.
White, R.W., Powell, R., 2010. Retrograde melt–residue interaction and the formation of near-anhydrous leucosomes in migmatites. Journal of Metamorphic Geology 28, 579–597.
White, S.H., Burrows, S.E., Carreras, J., Shaw, N.D., Humphreys, F.J., 1980. On mylonites in ductile shear zones. Journal of Structural Geology 2, 175–187.
Wiebe, R. A., Blair, K. D., Hawkins, D. P. & Sabine, C. P. 2002. Mafic injections, in situ hybridization, and crystal accumulation in the Pyramid Peak granite, California. Bulletin of the Geological Society of America 114, 909–20.
Wiebe, R. A. & Collins, W. J. 1998: Depositional features and stratigraphic sections in granitic plutons: implications for the emplacement and crystallisation of granitic magmas. Journal of Structural Geology 20, 1273–89.
Yakymchuk, C., Brown, M., Ivanic, T.J., Korhonen, F.J., 2013. Leucosome distribution in migmatitic paragneisses and orthogneisses: A record of self-organized melt migration and entrapment in a heterogeneous partially-molten crust. Tectonophysics 603, 136–154.
Yoshinobu, A. S. & Hirth, G. 2002. Microstructural and experimental constraints on the rheology of partially molten gabbro beneath ocean spreading centers. Journal of Structural Geology 24, 1101–7.
Závada, P., Schulmann, K., Konopásek, J., Ulrich, S., Lexa, O., 2007. Extreme ductility of feldspar aggregates—Melt-enhanced grain boundary sliding and creep failure: Rheological implications for felsic lower crust. Journal of Geophysical Research: Solid Earth, 112(B10).
Závada, P., Schulmann, K., Racek, M., Hasalová, P., Jeřábek, P., Weinberg, R. F., Štípská, P., Roberts, A., 2018. Role of strain localization and melt flow on exhumation of deeply subducted continental crust. Lithosphere 10, 217–238.
Zhang, W.Q., Liu, C.Z., Dick, H. J., 2020. Evidence for multi-stage melt transport in the lower ocean crust: The Atlantis bank gabbroic massif (IODP Hole U1473A, SW Indian Ridge). Journal of Petrology 61, egaa082.
Zhang, W.Q., Dick, H.J., Liu, C.Z., Lin, Y.Z., Angeloni, L.M., 2021. MORB Melt Transport through Atlantis Bank Oceanic Batholith (SW Indian Ridge). Journal of Petrology 62, egab034.
Zibra, I., Gessner, K., Smithies, H.R., Peternell, M., 2014. On shearing, magmatism and regional deformation in Neoarchean granite-greenstone systems: insights from the Yilgarn Craton. Journal of Structural Geology 67, 253–267.

Figure Captions

Figure 1 Field characteristics of mylonitic high-strain zones formed by solid-state deformation include compositional banding, fabric gradients adjacent to the high-strain zones, changes in colour, grain size reduction, new foliation and lineation and deflection of pre-existing foliation or layering. Note also outcrop-scale boudin, S-C’ fabric, mantled porphyroclasts and bimodal grain sizes. (a,b) greenschist facies, Glencoul and Arnaboll thrusts, Scotland; (c) greenschist to amphibolite facies Caswell Thrust, Caswell Sound, Fiordland, New Zealand (Daczko et al., 2002a); (d,e) Anita Shear Zone, Milford Sound, Fiordland, New Zealand (Klepeis et al., 1999; Gardner et al., 2015); (f) Wongwibinda Shear Zone, Southern New England Orogen, NSW, Australia (Craven et al., 2013; Jessop et al., 2020). For typical microstructures, see Figures 3 and 5.

Figure 2 Field characteristics of amphibolite to granulite facies high-strain melt migration pathways (i.e., zones of deformation-assisted migration of an externally derived melt) include compositional banding, fabric gradients adjacent to the high-strain zones, changes in colour, grain size reduction, new foliation and lineation and deflection of pre-existing foliation or layering, with or without recognisable igneous components. (a,b) Mt Daniel dyke and sheet complex emplaced into the active Mt Daniel Shear Zone, Mt Daniel, Fiordland, New Zealand (Daczko et al., 2002b; Bhattacharya et al., 2018), (c) Pembroke Thrust, Pembroke Valley, Fiordland, New Zealand (Daczko et al., 2001; Stuart et al., 2018a,b), (d,e) Hawes Head shear zone, Hawes Head, Fiordland, New Zealand (Daczko et al., 2012), small cross-cutting shear zone in the Doubtful Sound Shear Zone, Doubtful Sound, Fiordland, New Zealand (Gibson et al., 1988). For typical microstructures, see Figures 4 and 5.

Figure 3 Field and microstructural characteristics of banded mylonitic high-strain zones (between dashed lines); (a) greenschist facies, Moine Thrust, Lake Eriboll, Scotland; black lens cap for scale (60 mm across); (b) upper greenschist to lower amphibolite facies mylonite zone, with bent earlier foliation (white line), Cap de Creus, NE Spain; chisel (17 cm long) for scale; (c) amphibolite facies, Caswell Sound Thrust, New Zealand; marker pen (14 cm long) in inset for scale.

(Subscript i in each column) overview photomicrographs in plane (upper) and crossed (lower) polarised light; FOV = 2.8 cm; **(subscript ii and iii in each column)** close-up photomicrographs; crossed polarised light showing (a_{ii}) elongate, asymmetric porphyroclasts of quartz embedded in fine grained matrix; note strong undulose extinction, (a_{iii}) bimodal grain size distribution with matrix of fine grains, (b_{ii}) fractured feldspar, (b_{iii}) highly elongate ribbons of quartz embedded in fine-grained matrix of feldspar and quartz; note the undulose extinction (white arrow) of the quartz ribbons, (c_{ii}) bent twins (white arrow) in feldspar, (c_{iii}) micro-fractures (white arrow) in feldspar.

(Bottom panels) Summary table of field and microstructural characteristics of mylonite.

Figure 4 Field and microstructural characteristics of amphibolite to granulite facies high-strain melt migration pathways (i.e., zones of deformation-assisted migration of an externally derived melt) with some (a) to very little (b,c,d) outcrop evidence for the former presence of melt, i.e., the high-strain zones lack domains of felsic, coarse grained (leucocratic) material; black lens cap for scale (60 mm across). (a) Gough Dam shear zone, Central Australia (Piazolo et al., 2020; Silva et al., 2022); inset shows a cm-scale felsic component with igneous microstructure (i.e., granite lenses) and biotite (Bt) selvages; (b) Cattle water pass shear zone, Central Australia (Ghatak et al., 2022); anastomosing Grt-Bt (garnet-biotite)-rich foliation; inset shows partially replaced coarse ancient garnet and isolated K-feldspar grains; (c, d) Pembroke Valley, New Zealand; pre-existing foliation (S_1) and dykes deflected (white line) into high-strain zones with new foliations (S_2, dashed line); note the colour change in the high-strain zones; **(Subscript i in each column)** overview photomicrographs in plane (upper) and crossed (lower) polarised light; FOV = 2.8 cm; (subscript ii, iii, iv and v in each column) close-up photomicrographs and BSE (back-scattered electron) images with 100μm scale bars showing: (1) key microstructures of the former presence of melt: euhedral or faceted grains (white lines, a_{ii}, a_{v}, b_{iii}); grains displaying interstitial texture (a_{ii}–d_{iv}), including grains with low dihedral angles (yellow arrows) and elongate single grains that are inferred to have pseudomorphed melt films (white arrows); several closely-spaced xenomorphic grains with the same orientation that represent single grains connected along grain boundaries and triple junctions in three dimensions (green arrows) – in the examples shown, the xenomorphic grains are interstitial to biotite (a_{iii}) and garnet (b_{ii}), crossed polarised light with the two polarisers at 75°); pseudomorphed melt pockets (i.e., fine-grained, intergrown, multiphase aggregates of quartz-feldspar, a_{iii}, c_{v}, d_{iii}, d_{iv}); and quartz-feldspar-rich "veins" at a high-angle to the foliation, defined by trains of quartz, feldspar and amphibole grains forming a string-of-beads texture (black arrows, d_{ii}). (2) melt-mediated coupled dissolution-precipitation reaction textures (orange arrows) where pre-existing grains (e.g., Grt, garnet, in b_{iv} and b_{v}, and Cpx, clinopyroxene, in c_{ii}) are partially replaced at grain margins and along dissolution channels and/or fractures. Note that fractures in b_{v} are filled with Bt+Sil+Pl, biotite + sillimanite + plagioclase, the same reaction replacement assemblage observed at grain margins. Also note that pre-existing garnet is decorated with many fine-scale trails of porosity (black in BSE) consistent with former melt-filled porosity, a key indicator of coupled dissolution-precipitation. (3) rare porphyroclasts (c_{ii}, c_{iii}).

(Table) Summary table of field and microstructural characteristics of rocks formed in high-strain melt migration pathways (i.e., zones of deformation-assisted migration of an externally derived melt).

Figure 5 Schematic diagram showing the geometry and key features of high-strain zones with a focus on microstructural characteristics that distinguish high-strain rocks formed in (I) mylonite zones from (II) those rocks formed in high-strain melt migration pathways (i.e., zones of deformation-assisted migration of an externally derived melt), here called 'melferite'. See text for discussion. Note many of the microstructural features of mylonitic rocks deformed in the solid state are asymmetric and useful indicators of the sense-of-shear. This asymmetry is less common in melferitic rocks. Schematic diagrams modified after Passchier and Trouw, 2005, Cesare et al., 2009; Holness & Vernon, 2015; Stuart et al., 2018a; and Meek et al., 2019. Note that some features such as (5I, a) marker and foliation deflection, and (5I, j) lattice preferred orientation are also possible in melferite (5II).

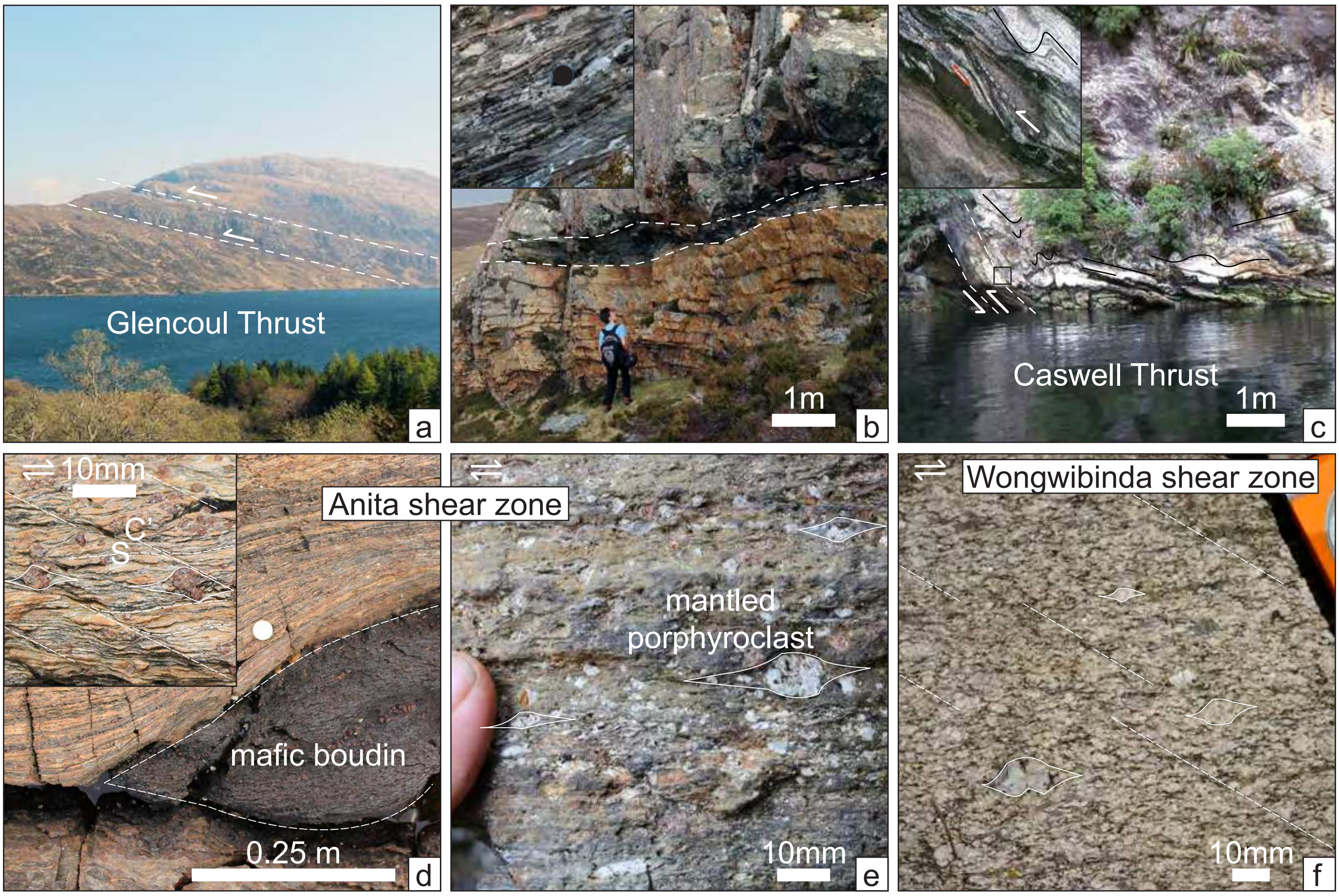

Daczko & Piazolo
Figure 1

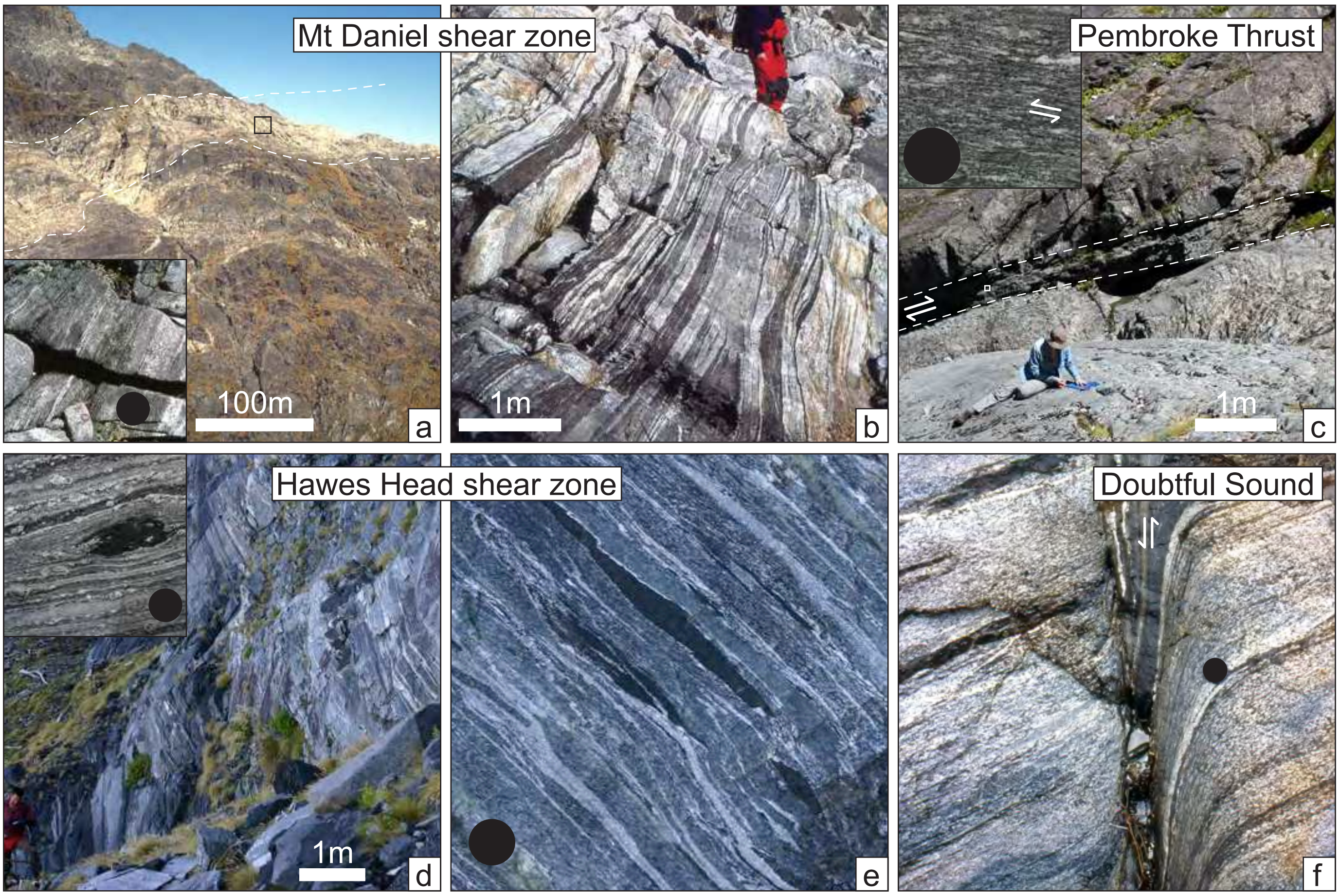

Daczko & Piazolo
Figure 2

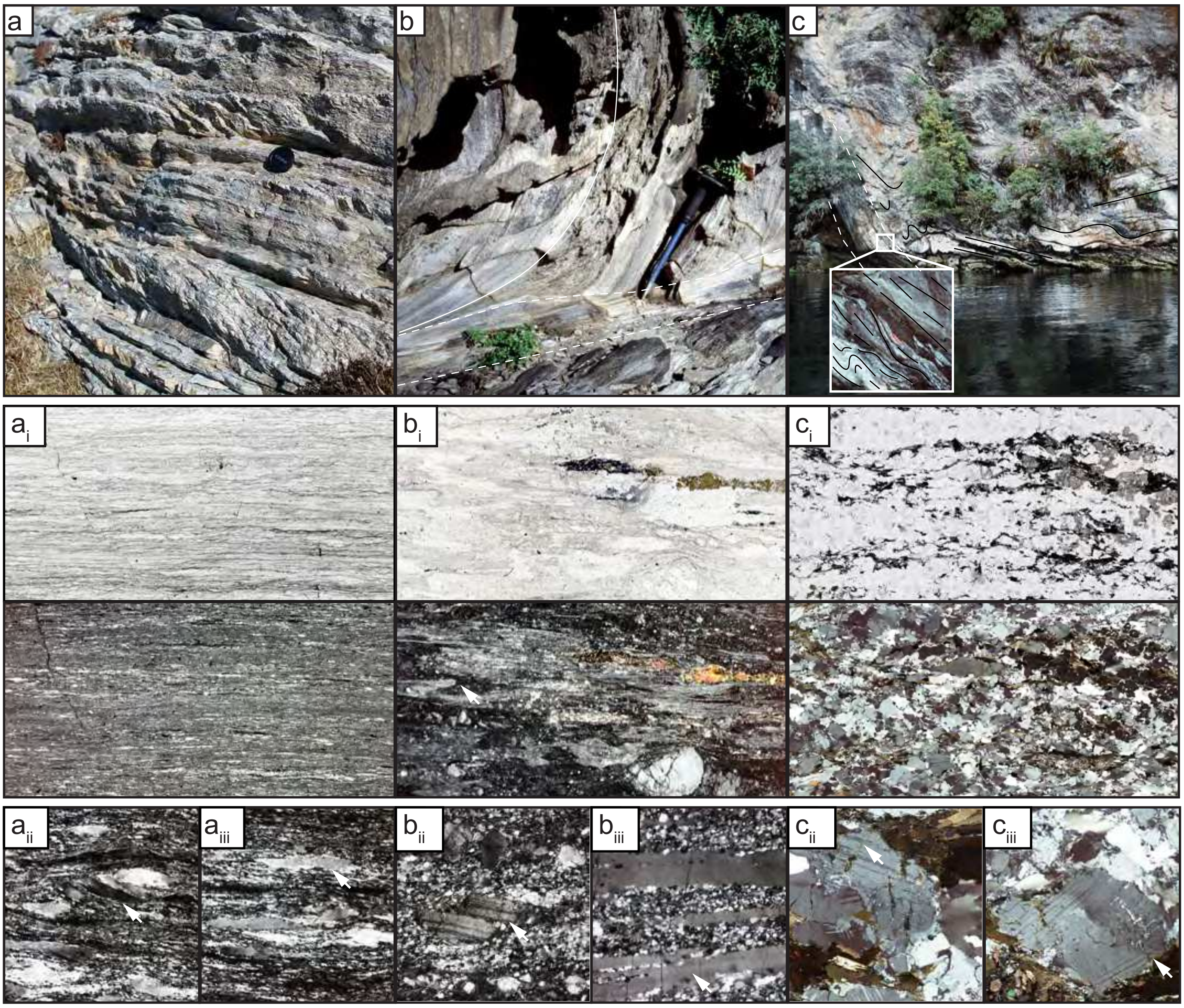

Characteristics of mylonite	
Field	**Microstructural**
Compositional banding	Bimodal grain size distribution
Fabric gradient adjacent to the high strain zone	Matrix of small dynamically recrystallised grains
Change in colour	Elongate porphyroclasts with undulose extinction, subgrains, & deformation lamellae and twins
Grain size reduction	Core-and-mantle structure
New foliation and lineation	Curved–highly irregular grain boundaries
Deflection of pre-existing foliation or layering	Window & pinning structures
	Shape-preferred and/or lattice-preferred orientation
	Micro-folding, shear bands, & asymmetric microstructures
	Brittle and ductile deformation

Daczko & Piazolo
Figure 3

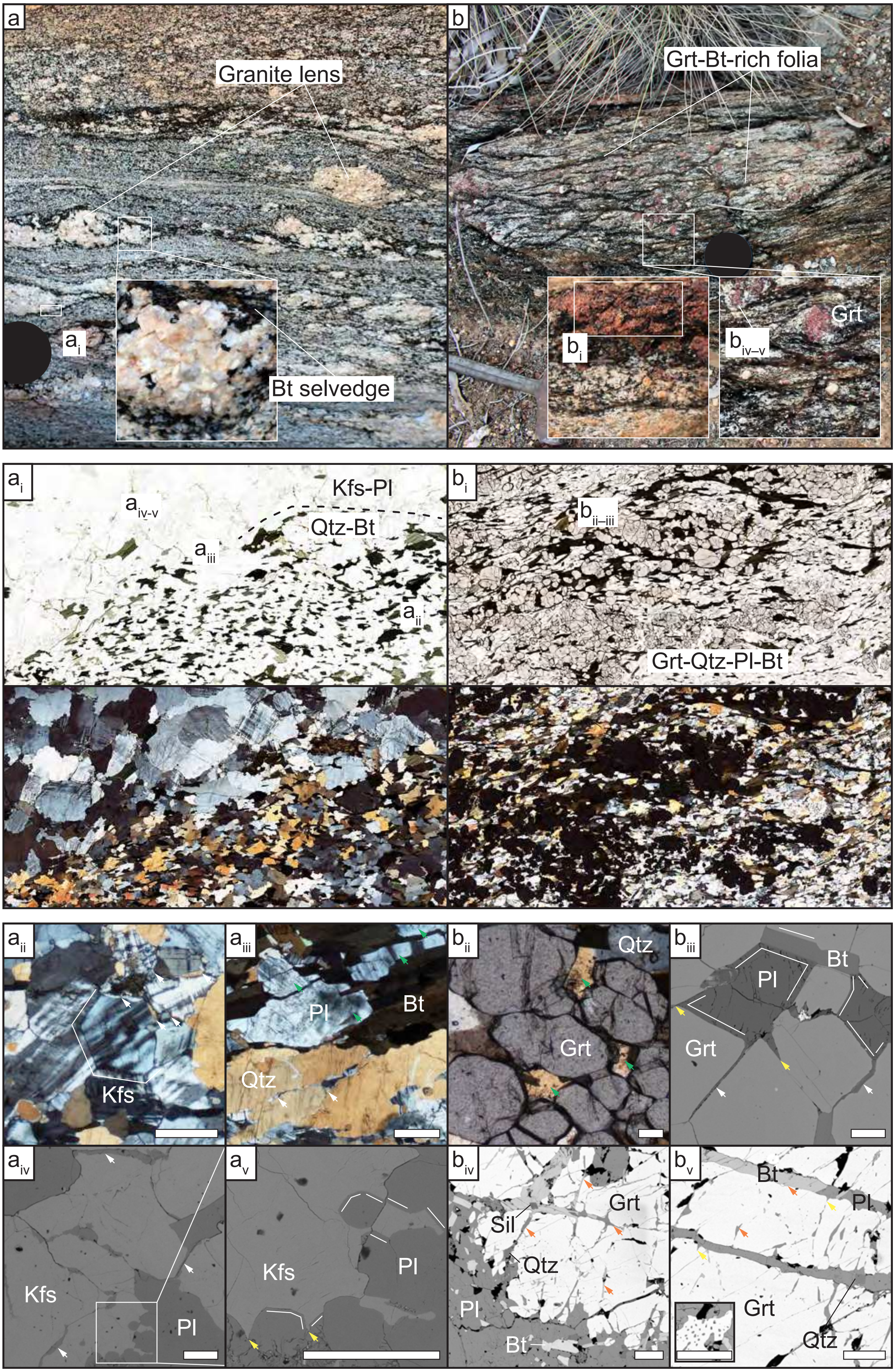

Daczko & Piazolo
Figure 4 (Part 1)

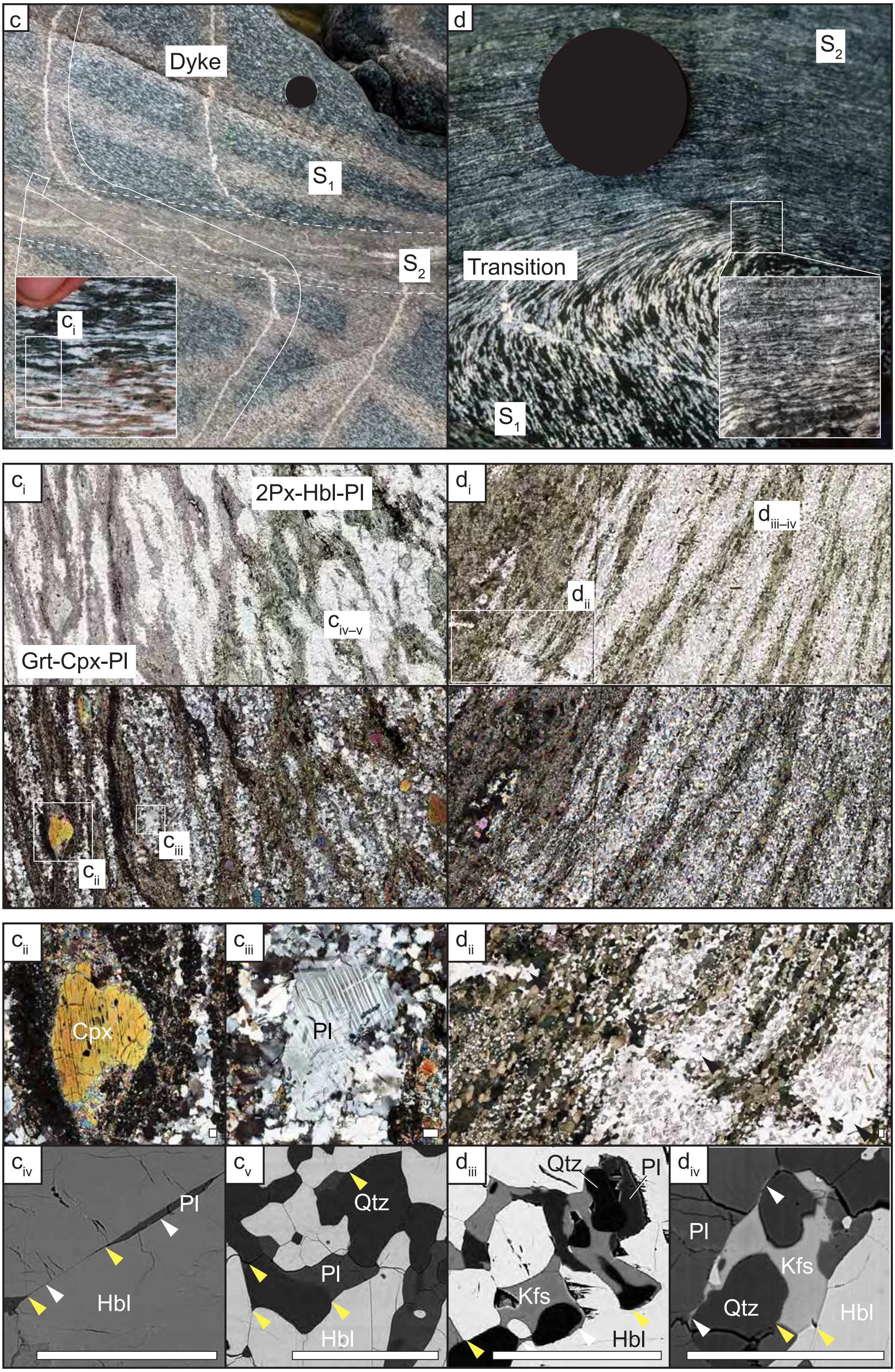

Daczko & Piazolo
Figure 4 (Part 2)

Characteristics of Melferite		
Field	Microstructural	
Compositional banding Fabric gradient adjacent to the high strain zone Change in colour Grain size reduction New foliation and lineation Deflection of pre-existing foliation or layering ***With or without recognisable igneous component***	Dominantly unimodal grain size distribution Limited matrix of small dynamically recrystallised grains Few porphyroclasts; grains largely lack (i) undulose extinction, (ii) subgrains, & deformation lamellae and (iii) twins Rare core-and-mantle structure Shape-preferred or lattice-preferred orientation Micro-folding, shear bands, & asymmetric microstructures are less common	***Microstructures indicative of the former presence of melt:*** - Some euhedral &/or faceted grains - Interstitial texture - Grains with low dihedral angles - Xenomorphic grains connected along grain boundaries & triple junctions in 3D. - Pseudomorphed melt films (extremely elongate single grains), - Pseudomorphed melt inclusion or pocket (fine-grained, intergrown, multiphase aggregates)

Daczko & Piazolo
Figure 4 (Part 3)

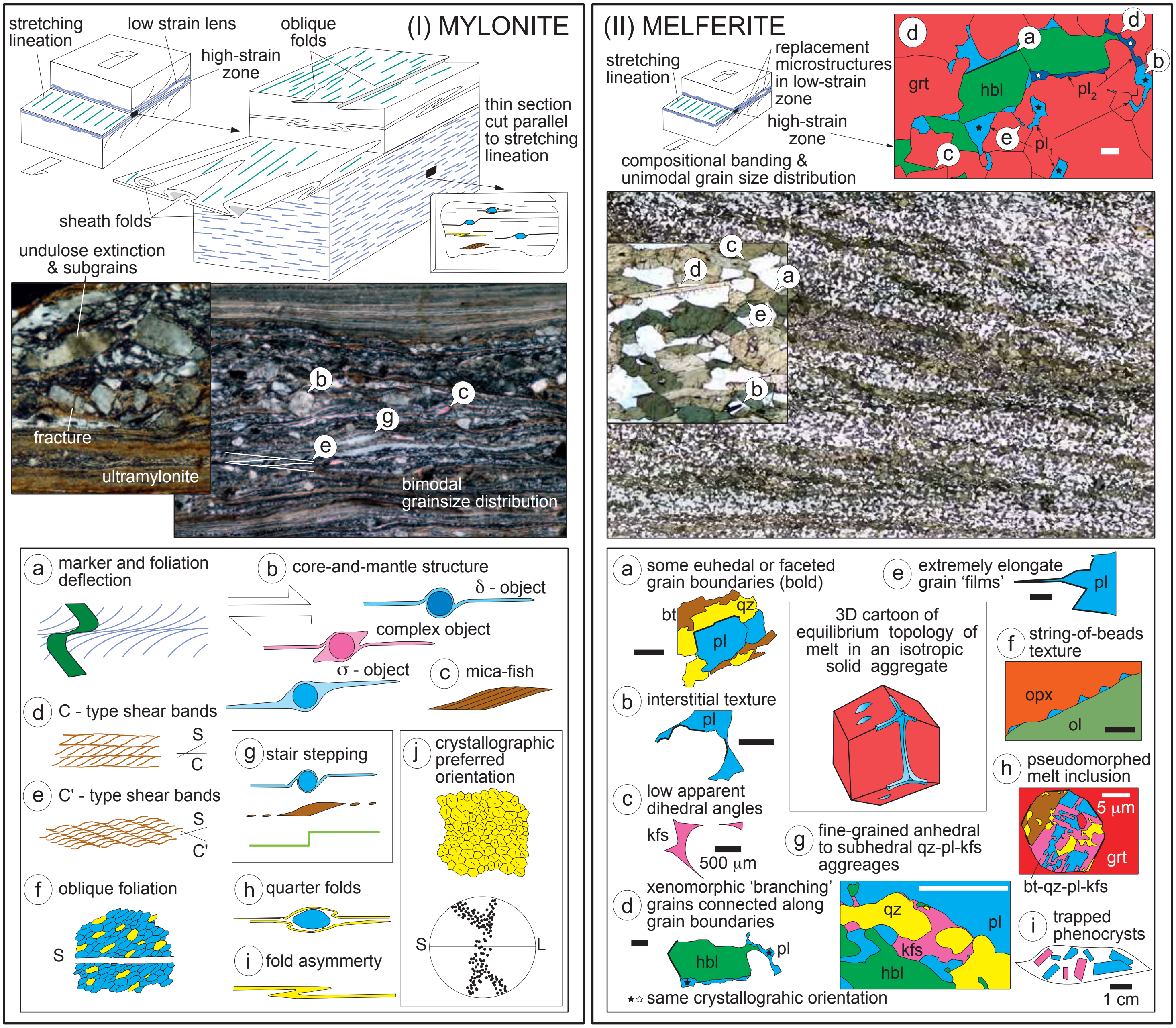

Daczko & Piazolo
Figure 5